

**UNIVERSITY OF ESSEX SCHOOL OF LIFE  
SCIENCES RESEARCH PROJECT, MSD  
MARINE BIOLOGY**

**Project title: Light hydrocarbon ratios as  
biosignatures of microbial activity**

**Leslie Ian Galstaun**

**ligals@essex.ac.uk**

**Supervisors: Dr. Michael Steinke & Prof. Terry McGenity**

**Date: 21/10/2020**

**Word count: 19962**

## **Contents**

<b>Acknowledgements</b> .....	4
<b>Abstract</b> .....	5
<b>Chapter 1 – Literature review</b> .....	6
1.1 <i>Methanogen microbiology</i> .....	6
1.2 <i>Methane production in oxic environments</i> .....	9
1.3 <i>Isotope systematics of carbon and hydrogen</i> .....	11
1.4 <i>Light hydrocarbons as tracer gases</i> .....	13
1.5 <i>Biosynthesis of higher hydrocarbons</i> .....	14
1.6 <i>Global hydrocarbon sinks</i> .....	18
1.7 <i>Methanogenic biosignatures and applications in astrobiology</i> .....	20
1.8 <i>Research aims</i> .....	24
<b>Chapter 2 - Methods development</b> .....	27
2.1 <i>Introduction</i> .....	27
2.1.1 <i>Sampling strategy</i> .....	27
2.1.2 <i>Real time spectroscopy for methane analyses</i> .....	30
2.2 <i>Methods</i> .....	31
2.2.1 <i>In-situ flux analysis</i> .....	31
2.2.2 <i>Physical measurements</i> .....	32
2.2.3 <i>Calibrations</i> .....	36
2.2.4 <i>Statistical analysis</i> .....	37

2.3 Results .....	37
2.5 Discussion .....	43
<b>Chapter 3 – Methanogenesis in a temperate estuary</b> .....	<b>46</b>
3.1 Introduction .....	46
3.1.1 Methanogenesis in the River Colne .....	47
3.2 Methods .....	49
3.2.1 Field Sampling .....	49
3.2.2 Sediment incubations .....	50
3.2.3 Sediment water and organic content .....	50
3.2.4 Trace gas analysis in water and atmospheric samples .....	50
3.2.5 Dissolved nutrient determination in estuarine water samples .....	51
3.2.6 Statistical analysis .....	51
3.3 Results .....	52
3.3.1 General physico-chemical characteristics of the Colne Estuary .....	52
3.3.2 Dissolved methane and ethane concentrations in estuarine water samples .....	53
3.3.3 Ex-situ incubations .....	53
3.3.4 In-situ hydrocarbon fluxes .....	55
3.4 Discussion .....	63
3.4.1 Physico-chemical parameters and their effect on methanogenesis in the Colne estuary .....	63
3.4.2 Contextualising dissolved hydrocarbon dynamics in the Colne estuary .....	64
3.4.3 Hydrocarbon fluxes in the Colne Estuary .....	66
3.4.4 Sedimentary hydrocarbon production .....	67

<b>Chapter 4 – Summary</b> .....	69
<i>4.1 Conclusions based on findings from the study</i> .....	69
<i>4.2 Improvement suggestions for future studies</i> .....	70
<i>4.3 Summary</i> .....	71
<i>References</i> .....	73
<b>Appendix</b> .....	87

## **Acknowledgements**

I would like to acknowledge my supervisors, Dr. Michael Steinke & Prof. Terry McGenity, for their tireless support and providing me the opportunity to produce this thesis. I would also like to acknowledge the astrobiology team at the Open University, particularly Dr. Mario Toubes-Rodrigo and Prof. Karen Olssen-Francis, for their creative feedback and inspiration for many parts of this project. Further, I acknowledge the staff and students of the Prince of Songkhla University, Thailand, as well as NARIT for supporting research efforts.

I would like to acknowledge my friends, particularly Mia Hanlon, Jess Wright, Emma Ward and Will Spanner for their positivity, support, and feedback throughout the development of this thesis.

Finally, I would like to thank my parents and my sister for their never-ending support throughout this project. I truly am blessed to have them around.

## Abstract

The River Colne, UK, is a temperate estuary with large expanses of anoxic mudflats, referred to as a “microbial observatory”. Methane and ethane emissions were characterised over three sites spanning from the head of the estuary (Hythe), mid-estuary (Alresford) and the mouth (Mersea) which were sampled for dissolved hydrocarbons, *in-situ* fluxes, and hydrocarbon production from *ex-situ* sediment slurry incubations. Dissolved methane concentrations were highest at Mersea ( $85.88 \pm 17.36$  nM CH<sub>4</sub>) followed by Alresford ( $27.75 \pm 14.29$  nM CH<sub>4</sub>). Dissolved ethane concentrations at Hythe were highest with  $631.05 \pm 315.89$  pM, followed by Mersea ( $605.69 \pm 302.84$  pM), with Alresford dipping to 0 pM. Methane fluxes were highest at Hythe for both the sediment-air ( $56.37 \pm 12.40$  nM min<sup>-1</sup> cm<sup>-2</sup>) and water-air interfaces ( $134.73$  nM min<sup>-1</sup> cm<sup>-2</sup>). Sediment-air ethane fluxes at Hythe averaged  $439.91 \pm 19.98$  pM min<sup>-1</sup> cm<sup>-2</sup>, decreasing at Alresford ( $407.81$  pM min<sup>-1</sup> cm<sup>-2</sup>), while water-air at Hythe produced  $892$  pM min<sup>-1</sup> cm<sup>-2</sup>, double that of Alresford ( $483.22 \pm 388.71$  pM min<sup>-1</sup> cm<sup>-2</sup>) with no ethane fluxes at Mersea. Incubations from Hythe, Alresford and Mersea increased by  $55.67 \pm 72.094$ ,  $0.04 \pm 0.158$  and  $0.69 \pm 0.489$  mM d<sup>-1</sup> in headspace CH<sub>4</sub> while mean ethane concentrations were  $215.97 \pm 12.373$ ,  $141.10 \pm 59.839$  and  $182.86 \pm 66.897$  pM, respectively. Methane concentrations were significantly lower in slurries incubated with 2-bromoethanesulfonic acid (2-BES) or after autoclaving, while ethane concentrations were unaffected. These results, coupled with calculated methane – ethane ratios, can be used to inform future studies, particularly with regard to astrobiological research.

## Chapter 1 – Literature review

### 1.1 Methanogen microbiology

Methane (CH<sub>4</sub>) is a globally distributed atmospheric gas produced primarily from biological production, particularly via archaeal methanogenesis. Methanogenic Archaea are the only organisms known that produce methane as a side effect of their metabolic processes.

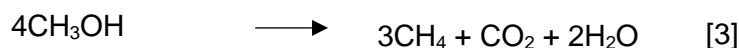
Methanogens are obligate anaerobes which metabolise in anoxic conditions, and are the focus of many global research efforts, due to CH<sub>4</sub> being a significantly radiatively active “greenhouse” gas. Greenhouse gases are compared in their global warming potential by converting to the equivalent amount of CO<sub>2</sub> (e.g. 1 kg of atmospheric methane is equivalent to 84 kg of CO<sub>2</sub>, although the atmospheric lifetime is shorter). Methane is increasing in tropospheric concentrations [1773.29 to 1860.2 ppb; CO<sub>2</sub>eq – 44.33 – 46.51 ppm (January 2010 – September 2018)] (Dlugokencky, 2018). Archaeal CH<sub>4</sub> is the primary source, contributing 80-90% of atmospheric CH<sub>4</sub> levels (Thebrath *et al.*, 1993).

Archaea were initially described as extremophiles, with different species adapted to radiation, acid, alkaline, salt, heat and pressure (Reed *et al.*, 2013). However, Archaea are also ubiquitous in less extreme environments, such as estuaries (Oremland *et al.*, 1981) and salt marshes (Bartlett *et al.*, 1987) and contribute to a significant portion of Earth’s biogeochemical cycles. Methanogens are strongly linked to agriculture and livestock production, producing significant amounts of the global CH<sub>4</sub> budget from habitats such as wetland crops (e.g. rice fields).

Traditionally, methanogens were phylogenetically restricted to the phylum Euryarchaeota, and made up five distinct classes (*Methanobacteria*, *Methanococci*, *Methanomicrobia*, *Methanopyri*, and *Thermoplasmata*), though recent evidence implicates methyl-reducing Archaea in non-euryarchaeal candidate phyla Verstraetearchaeota (Vanwonterghem *et al.*, 2016) and “Bathyarchaeota” (Evans *et al.*, 2015). Methanogens are among the most ancient organisms on Earth, with evidence for horizontal gene transfer between methanogens and cyanobacterial ancestors occurring over 3.51 billion years ago, though methanogenesis itself

may have evolved earlier (Wolfe and Fournier, 2018). Most methanogens typically fix inorganic carbon in the form of CO<sub>2</sub> into CH<sub>4</sub> through metabolic processes, which could have emerged as some of the first metabolic reactions alongside chemolithoautotrophy in deep sea hydrothermal vents (Martin *et al.*, 2008).

Methanogens are commonly classified with respect to the substrate they utilise for methane formation. Whiticar (1999) defines three common methanogenic groups: hydrogenotrophic (Equation 1), acetoclastic (Equation 2) and methylotrophic (Equation 3).



Substrates for methanogenesis are described as competitive and non-competitive, where the former refers to substrates which are used by other bacterial assemblages such as sulfate-reducing bacteria (SRB), which outcompete methanogens in sulfate-rich waters due to their higher affinity for H<sub>2</sub> and acetate (Kristjansson and Schönheit, 1983). Non-competitive substrates include the methylotrophic pathways, utilising compounds such as dimethyl sulfide (DMS) and mono-trimethylamines, which are not used by SRB. Methylotrophic methanogens become particularly relevant when considering hypersaline environments such as salt lakes, which contain a high concentration of terminal electron acceptors, particularly sulfate (Daffonchio *et al.*, 2006).

Hypersaline environments traditionally were assumed to reduce biodiversity due to the high desiccation pressure. Natural haloclines are created at brine-freshwater interfaces, frequently containing gradients of chemicals, including electron donors and acceptors which may enhance microbial diversity (Daffonchio *et al.*, 2006). This creates intense competition for competitive substrates, favouring the SRB over hydrogenotrophic methanogens, due to their higher affinity and energy yield from H<sub>2</sub>. Methylotrophic methanogens take advantage of the often high concentrations of non-competitive substrates such as methylamines which

are synthesised from compatible solutes (e.g. glycine betaine) utilised by other microbes (McGenity and Sorokin, 2018), leading to a dominance of methylotrophic methanogens such as *Methanohalophilus* in hypersaline environments.

Acetate, methylamine and hydrogen are typical methanogenic substrates which are cycled through a complex consortium of other microorganisms. Syntrophy is essential in anaerobic conversion of organic matter to methane, where metabolically distinct microorganisms are tightly linked by the need to maintain exchanged metabolites at low concentrations (McInerney *et al.*, 2009). Methanogens have a high affinity for these substrates, which are often produced through degradation of fatty acids by syntrophic organisms, which becomes energetically unfavourable unless the end products are used by methanogens and maintained at a low concentration. Methanogens are often difficult to culture due to this tight coupling with other syntrophic organisms. The lineage rice culture I, which are the most abundant and active members of the methanogenic community inhabiting rice paddy soils (Lu and Conrad, 2005) could only be cultured after an enrichment protocol was devised that included a syntrophic propionate degrader (*Syntrophobacter fumaroxidans*) to allow continuous hydrogen production at very low partial pressures (Sakai *et al.*, 2007).

Hydrogenotrophic methanogenesis in sulfate rich ( $> 200 \mu\text{M}$ ) water columns or sedimentary pore fluids is severely restricted as SRB outcompete the methanogens for carbon substrates or available hydrogen, leading to low  $\text{CH}_4$  concentrations ( $< 0.5 \text{ mM}$ ) (Whiticar, 1999).

However, deeper sediments may have depleted sulfate concentrations, increasing overall dissolved  $\text{CH}_4$  concentrations, while methyl-reducing methanogens can continue to produce methane uninhibited by the activity of SRB.

Freshwater environments (that typically display low sulfate concentrations) facilitate methanogenesis once anoxic conditions are established in the sediments, with ~70% of methanogenesis occurring via the acetotrophic pathway (Takai, 1970). Typically, freshwater lakes accumulate  $\text{CH}_4$  in the anoxic hypolimnion during stable stratification which breaks

down during the autumnal mixing events, emitting 46% of the stored methane and 80% of the lake's annual diffusive methane emissions to the atmosphere (Fernández *et al.*, 2014).

### 1.2 Methane production in oxic environments

Biogenic methanogenesis is a topic of controversy in microbiology and atmospheric chemistry, as the process is typically inhibited by oxygen and higher concentrations of sulfates, which facilitates competition from SRB. However, a significant portion of the global methane budget arises from oxic, sulfate-rich marine surface waters. Net microbial oxidation of methane results in methane undersaturation throughout most of the oceanic water column, though near-surface waters are often 5-75% supersaturated compared to the atmosphere (Karl *et al.*, 2008). Coastal additions of methane from sediment, rivers and other methanogenic habitats may explain near shore supersaturation. However, pelagic systems are often supersaturated with oxygen relative to the atmosphere, which should not favour methanogenesis, leading to an apparent paradox termed the "Ocean methane paradox", confounding current understanding of methanogenesis.

Oremland (1979) describes methanogenic activity in plankton sampled from 10 m depth in the San Francisco Bay area after incubation with a cysteine-sulfide reducing agent, with CH<sub>4</sub> production inhibited by the addition of 2-bromoethanesulfonic acid (BES), a now widely used methanogenic inhibitor. Samples from fish intestines were also extracted and enriched in methanogen growth media, testing positive for methanogen presence, suggesting zooplankton and fish intestines provide anoxic microenvironments where methanogenesis can occur in oxic and sulfate-rich waters while avoiding direct competition with SRB.

Karl *et al.* (2008) discovered aerobic degradation of methylphosphonate (MPn) by bacteria (e.g. *Trichodesmium erythraeum*, a cosmopolitan nitrogen fixing organism) produces CH<sub>4</sub>. Aerobic production of methane from MPn-amended seawater samples containing *T. erythraeum* reached 28.4 nmol L<sup>-1</sup> CH<sub>4</sub>. Unfiltered seawater samples collected from the Sargasso Sea produced ~ 1.0 μM CH<sub>4</sub> after addition of 1 μM MPn, while samples amended with only phosphorus produced no methane. Karl *et al.* suggest that if 1-2% of the net

organic P flux was cycled through MPn, it could reconcile the ocean methane paradox while also suggesting the availability of phosphate regulates methane production in oligotrophic waters. Phosphate availability in the photic zone is largely controlled through upwelling of high nutrient, deep waters. The expansion of ocean areas displaying oligotrophic conditions ( $0.8 - 4.3\% \text{ year}^{-1}$ ) (Polovina *et al.*, 2008) coupled with increased vertical water stratification due to ocean warming will therefore disrupt flux of marine  $\text{CH}_4$  to the atmosphere.

Repeta *et al.* (2016) expanded on the work of Karl *et al.* (2008) by using nuclear magnetic resonance to show that polysaccharide esters of three phosphonic acids present in dissolved organic matter are degraded by bacterial activity to create methane, ethylene and propylene, while also suggesting that daily cycling of only 0.25% of the phosphonic inventory in the test site could account for all atmospheric methane flux. The apparent paradox could therefore be explained by physical anoxic refuges in macroorganisms such as fish intestines and by aerobic degradation by bacteria, particularly nitrogen fixing organisms (e.g. *T. erythraeum*).

Freshwater systems show a similar apparent paradox. Epilimnetic, oxic waters showed supersaturation of  $\text{CH}_4$  relative to the atmosphere, with suggestions of anoxically produced, near-shore transport of  $\text{CH}_4$  or summer stratification breakdown responsible for residual  $\text{CH}_4$  in the oxic epilimnion (Schmidt and Conrad, 1993). Grossart *et al.* (2011) observed methane production in oxic epilimnetic waters in both unamended lab incubations and in-lake samples. Unamended water samples showed positive methane production, particularly in samples from the upper 8 m where cyanobacteria and microalgae were abundant, though additions of MPn had no effect. In-lake water samples were collected from different depths and removed excess methane through vigorous shaking, then incubated at the original depth *in-situ* in gas tight bottles exposed to light, darkness or with added 2-BES ( $>10^{-4} \text{ M}$ ), finding the highest average production rates at  $1.2 - 1.8 \text{ nM}\cdot\text{h}^{-1}$  at 6 m depth, with no significant differences in production between light and dark conditions. Microbial enrichment cultures produced from lake water samples were used as inoculants for axenic photoautotroph cells,

finding significantly higher methane production under well-oxygenated conditions compared to those conditions without the inoculum or the inoculum alone. Fluorescent *in-situ* hybridization (FISH) imaging revealed direct attachment of potentially methanogenic archaea to the photoautotroph cells. Photoautotrophs produce H<sub>2</sub> both through direct and indirect photolysis (Redwood *et al.*, 2009) while cyanobacteria can produce H<sub>2</sub> through nitrogen-fixing activities at night (Conrad and Seiler, 1980), suggesting photoautotrophs may directly be providing hydrogenotrophic methanogens with H<sub>2</sub>, facilitating oxic methanogenesis. Many methanogens can tolerate oxic conditions with genera such as *Methanosarcina* and *Methanocella* actively transcribing the *mcrA* gene and several ROS detoxifying genes, such as the *kat* (catalase) gene, which could allow certain genera of methanogens to tolerate oxic conditions in return for steady substrates provided by photoautotrophic plankton.

Yao *et al.* (2016) found evidence for methane production through demethylation of small organic compounds in a metagenomic study of a phosphorus-depleted lake system, finding enriched levels of the *phnJ* gene, which codes for the enzyme related to CH<sub>4</sub> production through cleavage of the C – P bond (alpha-D-ribose 1-methylphosphonate 5-phosphate C-P lyase). Phosphorus represses CH<sub>4</sub> production, suggesting P-starved microorganisms may be using demethylation of methylphosphonates as a source of phosphorus, supported by widespread distribution of the *phnJ* gene in methane-rich lakes.

These studies suggest freshwater systems and marine systems may host similar mechanisms of CH<sub>4</sub> production in oxic environments, though freshwater lakes will have more mixing of anoxic hypolimnion and oxic epilimnetic water during summer mixing events, facilitating transport of CH<sub>4</sub> more so than it is possible in marine environments.

### 1.3 Isotope systematics of carbon and hydrogen

Thermogenic CH<sub>4</sub> is typically produced through thermal decomposition of sedimentary organic matter, particularly type II and III kerogens, at high temperatures (157 – 221 °C) and pressures (Stolper *et al.*, 2014). “Natural gas” is produced through this process, which is primarily CH<sub>4</sub> in composition, along with smaller amounts of higher-chain hydrocarbons such

as ethane ( $C_2H_6$ ) and propane ( $C_3H_8$ ) as well as trace contaminants (e.g. hydrogen sulfide). Natural gas is heavily exploited globally for fuel, energy and household uses, and is extracted through hydraulic fracturing (“fracking”), making distinguishment between thermogenic and biogenic  $CH_4$  important for many sectors, particularly when searching for new reservoirs of natural gas.

Stable isotopes provide deeper understanding of sources of hydrocarbons. Stable carbon isotope values ( $\delta^{13}C$ ) are relative to the Vienna Pee Dee Belemnite standard, commonly expressed in per mille (‰) units. A similar systematic approach can be used for hydrogen where the ratios are amended to ( $H_2/H_1$ ) or more commonly abbreviated to  $\delta D$ , relative to standard mean ocean water (SMOW).

Thermogenic  $CH_4$  is generally enriched in  $^{13}C$ , ranging in  $\delta^{13}C_{CH_4}$  from -50 to -20‰, whereas biogenic  $CH_4$  values can reach as low as -100‰ (Whiticar, 1999). Isotope systematic dissimilarity between biogenic and thermogenic  $CH_4$  arises from differences in precursor compounds, magnitude of kinetic isotope effects and the relatively high temperatures required for thermogenic generation of hydrocarbon compounds. C-isotopic signatures of -20 to -80‰ are often cited as indicators of biogenic production, though much evidence suggests  $^{13}C$  information can only be a biosignature if it is accompanied by information on the  $^{13}C$  content of the precursor compounds (Whiticar, 1999; Xie *et al.*, 2013) and if additional fractionation through chemophysical processes does not occur or is accounted for (National Research Council, 2007).

Lower isotope mass compounds diffuse and react more quickly than heavier isotopes, leading to a preferential uptake of lighter isotopes by methanogens, resulting in strong depletion in  $^{13}C$  relative to precursor compounds. Kinetically controlled isotope fractionation is common in biology, and produces distinct signatures compared to equilibrium fractionation.  $\delta^{13}C$  isotope systematics can be combined with molecular information, such as ratios of light hydrocarbons ( $C_2/C_3$ ; see section 1.4) for more insightful discrimination between biogenic and thermogenic hydrocarbon production. Thermogenic  $CH_4$  (and  $C_2/C_3$

gases) produced by hydrogen-rich kerogen types I and II result in relatively low  $\delta^{13}\text{C}_{\text{CH}_4}$ , confounding an isotope systematic approach to understanding sources of production. Isotope systematic methods are often expensive and complicated to perform, leading to a need for a simpler and more streamlined approach to determining sources of  $\text{CH}_4$ .

#### 1.4 Light hydrocarbons as tracer gases

Ethane is the most globally abundant non-methane atmospheric hydrocarbon, typically ranging in atmospheric concentrations from 500 – 2200 ppt (Simpson *et al.*, 2012), primarily produced anthropogenically from natural gas leakage (62%), biofuel burning (20%) and biomass burning (18%) along with geological sources, with total global emissions estimated at 11 – 15 Tg  $\text{a}^{-1}$  (Simpson *et al.*, 2012). Ethane is an important atmospheric pollutant, removed through interactions with the hydroxyl radical ( $\cdot\text{OH}$ ) in the presence of nitrogen oxides ( $\text{NO}_x$ ) to produce ozone, resulting in average atmospheric lifespan of around two months (Xiao *et al.*, 2008). Ethane depletes the hydroxyl radical budget in the troposphere, elongating the lifespan of atmospheric methane and enhancing its warming effects. Ozone ( $\text{O}_3$ ) is a widespread air pollutant, resulting in  $0.7 \pm 0.3$  million respiratory mortalities  $\text{year}^{-1}$  (Anenberg *et al.*, 2010) and has a negative effect on primary productivity and crop health (Ainsworth *et al.*, 2012). Ozone's effect on public health, along with methane's warming potential, highlights a need to constrain sources of ethane.

The co-emission of ethane alongside methane and higher hydrocarbons in natural gas sources, such as shale gas (Visschedijk *et al.*, 2018), makes it a useful diagnostic tool for constraining the source of methane. Biogenically produced gas can produce trace quantities of  $\text{C}_{2(+)}$  hydrocarbons (Oremland *et al.*, 1981; Hinrichs *et al.*, 2006; Xie *et al.*, 2013), though primarily consists of  $\text{CH}_4$  and  $\text{CO}_2$  (Schoell, 1980). Thermogenic gas has a greater fractionation of higher chain hydrocarbons, allowing methane-to-ethane ratios (MER), often reported as  $\text{C}_1/\text{C}_{2-4}$ , to be used for assessing the origin of methane, particularly between thermogenic and biogenic methane. Simultaneous measurements of higher hydrocarbons are relatively simple when already measuring methane, resulting in MER having widespread

usage in the petrochemical field (Table 1.1). Schoell (1980) suggested a gas composition of less than 0.5 mol% ethane and  $\delta^{13}\text{C}\text{-CH}_4$  values less than -64‰ were purely microbial in origin. Gases with MER >1000 are typically considered to be biogenic in origin, particularly when coupled with low (< -50‰)  $\delta^{13}\text{C}\text{-CH}_4$  values (Bernard, 1978; Schoell, 1980). Table 1 provides an overview of MER, highlighting the large difference in MER between thermogenic (Schwietzke *et al.*, 2014; Gvakharia *et al.*, 2017) and biogenic (Oremland *et al.*, 1981; Osborn and McIntosh, 2010) gases from both atmospheric and dissolved gas measurements. Osborn and McIntosh (2010) suggest >5% composition of higher chain hydrocarbons to be indicative of thermogenic formation, and used environmental factors as further constraints, suggesting high concentrations (>~1 mM) of alternative electron acceptors (e.g.  $\text{SO}_4$ ) and salinity (>2-4 M Cl) inhibit methanogenesis and can be used with MER as diagnostics for gas formation, though methylotrophic methanogenesis can occur in even hypersaline environments (McGenity and Sorokin, 2018).

### 1.5 Biosynthesis of higher hydrocarbons

Oremland *et al.* (1981) found ethanogenesis occurring in methanogens collected from anoxic estuarine sediment by incubating sediment slurries under hydrogen and analysing 500  $\mu\text{L}$  headspace samples using a gas chromatograph (GC) with a flame ionisation detector (FID). Oremland *et al.* (1981) propose coenzyme M (CoM), a low molecular weight cofactor found only in methanogenic archaea, as a precursor for ethane biosynthesis. Addition of ethyl-S-CoM (a structural analog to CoM) to sediment slurries stimulated ethane production 12-fold and ethylene production 2-fold, while also increasing  $\text{H}_2$  uptake (6.1 to 7.3 mmol / flask). Incubation of sediment slurries treated with and without ethyl-S-CoM revealed trace  $\text{C}_2\text{H}_6$  production without coenzyme M, with markedly increased production when treated. Addition of 2-BES inhibited all methanogenic activity, including those treated with ethyl-S-CoM.  $\text{C}_2\text{H}_6$  had an optimum production temperature of 40 °C while  $\text{CH}_4$  reached optimum production at 65 °C. Sediment slurries incubated at 4 °C and 80 °C substantially lowered hydrocarbon production. Enrichments grown on methanogenic media revealed ethane production, while

Table 1.1: Summary of observed  $C_1/C_{2+}$  ratios from various geochemical and biological papers. Where possible, original reported ratios are given, otherwise units were standardised between  $CH_4$  and  $C_{2+}$  measurements before calculating the ratio. For Schiwietzke *et al.* (2014), the medium emission scenario was assumed for all calculations.

$C_1/C_{2+}$	Emission source	Method of measurement	Reference
86.1	Global coal		
3.2	Global oil	Global bottom-up	
12.7	Global NG	inventory	Schwietzke <i>et al.</i> , 2014
89.1	UK coal	modelling of	
3.2	UK oil	natural gas	
12.7	UK NG	measurements	
1.1	Bakken shale		
11.6	Barnett shale	Aerial	
3.4	Denver basin	reconnaissance	Gvakharia <i>et al.</i> , 2017
2.5	Eagle Ford West	measurements	
2.3	Eagle Ford East		
11.3	Haynesville		
264166.7	Anoxic estuarine sediment	<i>Ex-situ</i> incubations	Oremland, 1981
24420.0	Organic rich shale		
9160.0	Organic rich shale	Water samples	Osborn & McIntosh, 2010
6831.0	Organic rich shale		

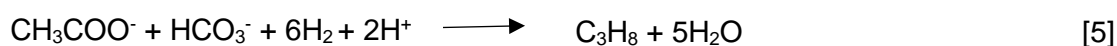
also being inhibited by 2-BES, suggesting a causal link between ethanogenesis and methanogenic activity. Ethyl-S-CoM is either biosynthesised or must be actively transported from the environment, suggesting ethanogenesis may require at least trace sulfur levels in the environment.

Ethane and propane have been found in cold marine sediments where contributions from thermogenic production is considered negligible (Hinrichs *et al.*, 2006). Hydrocarbon concentration decreases with distance from shore, though remains relatively constant with subseafloor depth (Bernard, 1978; Hinrichs *et al.*, 2006). These studies suggest biogenic production from microbial activity as C<sub>2</sub> and C<sub>3</sub> compounds were found in areas with temperatures too low for thermogenic production. Microbial production of ethane has an optimum temperature of 40 °C and is completely inhibited by temperatures above 80 °C in estuarine methanogens (Oremland *et al.*, 1981) while still being able to occur at 2 °C in deep sea sediments (Hinrichs *et al.*, 2006).

Previous evidence suggested that sorbed hydrocarbons in marine sediments are a result of fossil hydrocarbon reservoir seepages, demonstrating that sorbed hydrocarbons are relatively well protected from microbial degradation and could be preserved in sediments, while also observing elevated amounts of mature hydrocarbons and upward movement along tectonic lineaments (Knies *et al.*, 2004). Hinrichs (2006) found opposing evidence, collecting marine sediment cores from up to 380 m depth. Relatively low  $\delta^{13}\text{C}$  values for sampled hydrocarbons (C<sub>1</sub> = -60 ‰/C<sub>2/3</sub> = -20 ‰) provide strong evidence for biogenic production. Intact prokaryotic cells were found in all samples, with 16s RNA gene analysis revealing diverse assemblages of archaea and bacteria while chemical compositions of pore fluids indicated microbial activity at all depths. The study included sites geographically isolated from fossil hydrocarbons, where relatively thin packages of cold, organic-lean sediment overlay a basement through which oxygenated seawater circulates. C<sub>2</sub>/C<sub>3</sub> found in these samples must therefore have been produced *in-situ*, with the presence of dissolved

manganese, iron and sorbed methane with  $\delta^{13}\text{C}$  of  $<-65\%$  indicating microbial activity at all depths.

Claypool (1999) first suggested a mechanism through which biogenic ethane is formed from reduction of  $\text{C}_2$  acids in an analogous reaction to reduction of  $\text{CO}_2$  in reductive methanogenesis (Equation 4). Hinrichs (2006) provided geochemical evidence in support of this hypothesis, expanding to a scenario where condensation of dissolved inorganic carbon (DIC) to  $\text{C}_2$  compounds would lead to biogenic propane enriched in  $^{13}\text{C}$  (Equation 5), as sedimentary porewater is typically isotopically heavy, making determination of biogenic vs thermogenic hydrocarbon production via stable isotope analysis more complicated. Biogenic  $\text{C}_2/\text{C}_3$  production therefore provides a sink for fermentative products (acetate and hydrogen).



Xie *et al.* (2013) expanded on the previous work through exploring the ethane and propane producing potential of an ethanogenic enrichment in anoxic estuarine sediment, proposing ethylene reduction as a plausible explanation for ethane in cold marine sediments.

Experiments with ethyl-S-CoM revealed CoM as an enhancer of ethanogenesis, showing that the *mcrA* gene can target methanogenic communities in the environment (Oremland *et al.*, 1981). Xie *et al.* (2013) experimented with different  $\text{C}_2$  and  $\text{C}_3$  functional groups (alcohol, alkene and thiols) to assess the alkane production potential of each compound. Ethane formation was only observed in sediment incubated with ethylene and ethanethiol. They found incubation with acetate and high levels of  $\text{H}_2$  did not stimulate ethane production, disagreeing with Claypool (1999) and Hinrichs *et al.* (2006), refuting the “sink” hypothesis. All the substrates tested had poor potential for propane production, further refuting the hypothesis, finding only propanethiol producing propane at a low conversion efficiency (0.003%), comparable with lake sediments (0.002%) at the same propanethiol

concentrations (Oremland, 1988). 2-BES and sterilization inhibited propane formation, suggesting it is still microbially facilitated even if at a low conversion efficiency. Xie *et al.* (2013) posit that conversion of propylene to propane is not an intermediary step and that the enzymatic system involved in the conversion of ethylene to ethane does not have an analogous system involved in converting propylene to propane. Further experiments with varying H<sub>2</sub> partial pressures revealed ethylene reduction to ethane could be facilitated by concentrations as low as 0.01% H<sub>2</sub> (120 nmol L<sup>-1</sup> slurry), resembling concentrations found in some sedimentary environments (Lin *et al.*, 2012), suggesting high H<sub>2</sub> partial pressures in laboratory experiments are not necessary to stimulate ethylene to ethane production. C<sub>1</sub>/C<sub>2+</sub> ratios of 270-36000 from the ethylene enrichments showed a distinction from thermogenic natural gas (Table 1). Ethylene can be formed from cyanobacterial interaction with sulfate-reducing bacteria (Hodges and Campbell, 1998) in “black layer” sand through biofilm mediated anoxic conditions. Koene-Cottaar and Schraa (1998) propose ethane evolution from ethylene may be a detoxification mechanism in methanogens to adapt to toxic levels of ethylene, observing 100% reduction of ethylene to ethane in enrichment studies. Xie *et al.* (2013) suggest *Methanocalculus* as an ethanogenic archaea due to its hydrogenotrophic nature and use of acetate as a precursor. These studies provide evidence for ethanogenesis as a toxicological defense mechanism, adapting existing metabolic pathways used for methanogenesis. Propanogenesis may likely be an unintended side effect of this mechanism or perhaps an extension of it, though further research is still needed.

### 1.6 Global hydrocarbon sinks

Methane and the longer secondary hydrocarbons (C<sub>2</sub> – C<sub>5</sub>) share a major sink in the tropospheric hydroxyl radical ·OH, which accounts for oxidising 90% of the global CH<sub>4</sub> budget (Kirschke *et al.*, 2013) and around 95% of the ethane budget (Rudolph, 1995). Ethane particularly shows a strong interhemispheric gradient, equating to 11.8 Tg yr<sup>-1</sup> and 3.7 Tg yr<sup>-1</sup> turnover in the northern and southern hemispheres, respectively, balancing to a total removal of 15.5 Tg yr<sup>-1</sup> (Rudolph, 1995), correlating well with anthropogenic activities

(i.e. fewer industrial activities and people in the southern hemisphere).  $\cdot\text{OH}$  radicals are short lived ( $\sim 1$  s) and are formed mainly through photolysis of  $\text{O}_3$  and secondary radical propagation. Global tropospheric  $\cdot\text{OH}$  is not seasonally variable (Wolfe *et al.*, 2019) though does show strong seasonality when considering hemispheres independently, with both peaking in  $\cdot\text{OH}$  concentrations in mid-summer, along with a significant interhemispheric gradient (Wolfe *et al.*, 2019).

Hydroxyl radicals react with  $\text{CH}_4$  to produce the methyl radical  $\cdot\text{CH}_3$  and water vapour, which then progress through a complex series of reactions to produce  $\text{O}_3$  and water vapour, making methane oxidation an important source of tropospheric water vapour. Ethane reacts similarly, though produces distinct intermediates (e.g. acetaldehyde, acetic acid), making it important to tropospheric chemistry despite its trace atmospheric concentrations, opening up chemical pathways not accessible via methane oxidation alone (Rudolph, 1995). Methane and ethane exhibit seasonality in their atmospheric concentrations, predictably reversing the seasonal OH cycle with peaks in mid-winter and lows in summer (Rudolph, 1995; Saad *et al.*, 2016).

Globally, light hydrocarbons ( $\text{C}_1 - \text{C}_3$ ) have a large sink in microbially mediated aerobic oxidation, primarily by methanotrophic archaea and bacteria (Solomon *et al.*, 2007). Aerobic methanotrophy occurs using multiple pathways, classified as type I, II or X, which corresponds to the ribulose monophosphate (I) and serine (II) pathways for methane oxidation, and presence of ribulose-1,5-bisphosphate carboxylase (X). Type I and X methanotrophs belong to the *Gammaproteobacteria* whereas type II organisms belong to the *Alphaproteobacteria* (Hanson and Hanson, 1996). Globally, wetlands are a major sink for methane with type I and II aerobic methanotrophs catalyzing methane oxidation at the aerobic-anaerobic interface, which includes oxygenated surface soil and near oxygen-releasing wetland plant roots (Conrad, 2007). An estimated  $\sim 80\%$  of endogenous methane produced in anaerobic compartments (e.g. subsurface soil  $>10$  cm deep) is oxidised before escaping to the atmosphere (Conrad and Rothfuss, 1991). Less is known

about C<sub>2</sub> – C<sub>4</sub> aerobic biological oxidation, though methanotrophs from natural gas seeps have been observed oxidising C<sub>2</sub> – C<sub>4</sub> alkanes independent from C<sub>1</sub> oxidation (Kinnaman *et al.*, 2007).

Anaerobic oxidation of methane consumes 70 – 300 Tg CH<sub>4</sub> a<sup>-1</sup>, making it an important sink. Without this process, there would be 10 – 60% more atmospheric CH<sub>4</sub> (Conrad, 2009).

Anaerobic methane oxidation is categorised into three main pathways, namely the sulphate-dependent; nitrate/nitrite dependent and metal ion (Fe<sup>3+</sup>/Mn<sup>4+</sup>) dependent anaerobic methane oxidation pathways (Cui *et al.*, 2015). Sulphate-dependent anaerobic methane oxidation occurs mainly in marine and freshwater environments, while the nitrate/nitrite dependent pathway exclusively occurs in freshwater. The reverse is true for the metal ion dependent pathway, which occurs in marine environments (Cui *et al.*, 2015). Anaerobic oxidation of short-chain alkanes contributes significantly to community bioenergetics in marine ecosystems (Bose *et al.*, 2013), particularly in deep sea hydrothermal vents with natural gas seeps. Various studies have observed the anaerobic oxidation of short chain alkanes independent from methane oxidation (Kniemeyer *et al.*, 2007; Bose *et al.*, 2013), though it appears anaerobic ethane oxidation is orders of magnitude slower than C<sub>3</sub> – C<sub>4</sub> oxidation rates (Kniemeyer *et al.*, 2007). Short chain alkanes act as additional substrates for chemotrophic microbes in deep sea vents, alongside methane and other reduced organic and inorganic compounds.

### *1.7 Methanogenic biosignatures and applications in astrobiology*

Methanogenic hydrocarbon production can be used as a biosignature of microbial activity, particularly when considering the biogenic/thermogenic discriminating ratio of C<sub>1</sub>/C<sub>2+3</sub>.

Several studies have used gaseous hydrocarbons as biosignatures of microbial activity, particularly for use in the oil industry. Mode *et al.* (2014) used real-time gas chromatographic analysis of gaseous hydrocarbons (C<sub>1</sub> – C<sub>5</sub>) to characterise oil reservoir fluid dynamics, using ratios to characterise emissions for drilling purposes, while other studies combined

gaseous hydrocarbon ratios with isotope systematics to determine the nature of subsurface oil wells (Hammerschmidt *et al.*, 2014).

Gaseous hydrocarbon biosignatures are particularly relevant when discussing the exciting concept of extraterrestrial extremophilic archaea. Several detections of extraterrestrial methane have been reported (Oze and Sharma, 2005, Webster *et al.*, 2015), though the exact atmospheric abundances and sources are not clear. Methane has been detected on Mars primarily (Oze and Sharma, 2005; Webster *et al.*, 2015; Webster *et al.*, 2018), with additional detections on Enceladus, a moon of Saturn (Porco *et al.*, 2006; Waite *et al.*, 2006), though more recent evidence suggests there is little to no methane in the martian atmosphere (Yung *et al.*, 2018).

The Cassini spacecraft passed within 168.2 km of Enceladus and used its ion and neutral mass spectrometer to analyse an active atmospheric water vapour plume originating from a theorised subsurface saline ocean covered by a thick layer of ice in the southern hemisphere, finding CO<sub>2</sub>, H<sub>2</sub>O and methane at a mixing ratio of 1.63 – 1.68, as well as other trace compounds including propane and acetylene (<1%) (Waite *et al.*, 2006). Several other studies have confirmed the presence of methane in this plume (Dougherty *et al.*, 2006; Porco *et al.*, 2006), making it feasible that there could be methanogenic activity in the subsurface of Enceladus. The plume has been analysed on five further fly-bys by Cassini with better signal-to-noise ratios, making identification of benzene, definitive detections of NH<sub>3</sub> and probable presence of <sup>40</sup>Ar possible (Waite *et al.*, 2006). Ammonia lowers the boiling point of water to temperatures as low as -97.15 °C, and the presence of Na and K salts in E-ring (a micrometre thick ring of water vapour particles densest around Enceladus, postulated to originate from the subsurface ocean) ice particles in the plume suggest the presence of a subsurface salty ocean (Postberg *et al.*, 2009), which could be conducive to life. Steel *et al.* (2017) used the energy flux observed at the south pole and inferred internal hydrothermal activity to create a conceptual model of abiotic and biotic amino acid formation in the Enceladus subsurface ocean, postulating a H<sub>2</sub> production of 0.6 – 34 mol s<sup>-1</sup> from

serpentinization, enough to support  $1.6 - 87$  (abiotic) and  $1 - 44 \text{ g s}^{-1}$  (biotic) amino acid synthesis rates, which presents tolerable conditions for life to exist in. However, other evidence suggests methane may come from clathrate formation in the favourable conditions of the subsurface ocean, suggesting further research is necessary to discriminate between biogenic and abiotically produced methane (Bouquet *et al.*, 2015).

Methane detections on Mars are extensively documented and researched. *In-situ* direct ingestions from the Curiosity rover report an abundance of  $0.69 \pm 0.25$  ppbv (95% CI), with episodic elevated levels of  $7.2 \pm 2.1$  ppbv (95% CI) (Webster *et al.*, 2015). Remarkably, martian methane shows strong, repeatable seasonal variability (Fig. 1.1). The tuneable laser spectrometer on the Curiosity rover uses a two-channel system for *in-situ* atmospheric gas analysis, providing high spectral resolution. Webster *et al.* (2018) measured atmospheric  $\text{CH}_4$  at the Gale crater for five years, finding an average atmospheric  $\text{CH}_4$  concentration of  $0.41 \pm 0.16$  ppbv (95% CI) and a strong seasonal variability of  $0.25 - 0.65$  ppbv (Fig. 1.1). This variation is stronger than expected variation from the annual surface pressure cycle (see Fig. 1.1; solid black line) or from ultraviolet degradation of meteorically delivered organics, and also accounts for terrestrial contamination of  $\text{CH}_4$  in the digestion chambers of Curiosity, lending strong evidence to a biogenic source of  $\text{CH}_4$  on Mars. However, this data can be explained through abiotic processes, as Moores *et al.* (2019) show using numerical modelling with geological constraints that regolith adsorption and diffusion can reproduce the same seasonal variability if impregnated with  $\text{CH}_4$ , possibly from subsurface microseepages. Subsurface genesis of martian  $\text{CH}_4$  could lead to isotopic fractionation before atmospheric release due to  $^{12}\text{C}$  diffusing faster than  $^{13}\text{C}$ , with increased photochemistry on lighter  $^{12}\text{CH}_4$  leading to higher atmospheric loss compared to  $^{13}\text{CH}_4/\text{CH}_3\text{D}$  molecules (Nair *et al.*, 2005) causing naturally more negative  $\delta^{13}\text{C}$  ratios, masking potential methanogen biosignatures using this method.

Trace gas quantities of higher hydrocarbons in the martian atmosphere are not well understood. Krasnopolsky (2012) used the IRTF/CSHELL ground-based instrument suite to

detect ethane at  $0.0 \pm 0.8$  ppb in the martian atmosphere, with an upper limit of 0.2 ppb, suggesting ground-based measurements of martian hydrocarbons are not accurate enough to detect  $C_{2-n}$  in the trace quantities existing in the martian atmosphere. Synthetic spectra are used in ground-based telescopic observations to increase reliability of observations, mitigating effects of telluric contamination, and removing Fraunhofer lines. Errors associated with synthetic spectra fitting are common and affect reliability of ground-based measurements (Zahnle *et al.*, 2011).

Nadir and Occultation for Mars Discovery, or NOMAD, is part of the ExoMars Trace Gas Orbiter payload, launched in March 2016. NOMAD is a spectrometer suite measuring sunlight across a large spectrum, allowing for low-concentration atmospheric trace gas detection, eliminating many issues associated with ground-based telescopic observations. NOMAD collects large quantities of spectroscopic data in the martian atmosphere, offering an *in-situ* approach at a much higher resolution than previously possible. Korablev *et al.* (2019) report early findings from the orbiter from April to August 2018, finding an upper limit of 0.5 ppbv  $CH_4$  across multiple latitudes on both hemispheres, a figure 10-100 times lower than previously reported detections. This discrepancy in atmospheric methane to the higher figure reported from the Gale crater suggests an unknown process that can rapidly remove or sequester methane before it spreads globally (Korablev *et al.*, 2019).

Isotopic fractionation values for  $CH_4$  are well documented (Whiticar, 1999; Xie *et al.*, 2013) while  $C_2/C_3$  remains less understood, with some values found in marine sediments (Hinrichs *et al.*, 2006; Xie *et al.*, 2013).  $C_2/C_3$  ratios remain relatively unresearched in martian analogous environments (e.g hypersaline lakes). Camacho *et al.* (2017) studied Spanish hypersaline lake  $CH_4$  seasonal emissions using medium-term incubations of sediments *ex-situ*, while also recording the changes in  $CH_4$  headspace concentration.  $CH_4$  concentration was produced at markedly low rates in the hypersaline lakes compared to most temperate lakes, while also finding increased  $CH_4$  emissions at higher temperatures, varying expectedly

due to methanogen biology. No data were collected on C<sub>2</sub> or higher compounds, though it could be expected to follow a similar pattern at trace concentrations.

Methanogens are likely candidates for extra-terrestrial life on Mars and in other putative habitats on Enceladus and Europa, one of the Jupiter moons, as well as other extrasolar bodies due to their extremophile abilities and ecophysiological characteristics. Mars in particular appears to have possessed vast quantities of water in its Noachian period, although the low surface pressure currently means there cannot be liquid water on the planet's surface, although evidence for subsurface aquifers (Martínez and Renno, 2013) suggests an ideal habitat for methanogenic growth. Several studies have shown the survival potential of methanogens under simulated Martian-analogous conditions. Wagner *et al.* (2013) cultured *Methanosarcina soligelidi* SMA-21, a methanogenic archaeon isolated from Siberian permafrost, as a model organism and exposed cultures to various Martian-analogous conditions, including altering pH of the media from 4.1 – 9.9 using 1 M HCl and 1 M NaOH, altering ambient temperature from 0 to 64 °C and altering salinity from 0 to 0.6 M NaCl while measuring methane production via headspace injections using gas chromatography. Optimum growth conditions were found at 28 °C, 7.8 pH and 0.02 M NaCl. Further experiments involving exposing cell suspensions on microscope cover slides found high survival potential of strain SMA-21 against air exposure (up to 72 h), desiccation (up to 25 days), freeze–thaw cycles down to –78.5 °C and long-term freezing (up to 2 years at –20 °C). These results show the survivability of methanogens under a range of conditions, including Martian-analogous conditions, further suggesting their viability as extra-terrestrial candidates.

### 1.8 Research aims

The aim of this research is to quantify biogenic emissions of light hydrocarbons produced by methanogens in a range of environments and habitats, particularly with respect to salinity, to produce an inventory of C<sub>1</sub>/C<sub>2+3</sub> ratios to extend our current knowledge on methanogenesis along hypertrophic estuaries and to support future astrobiological studies, particularly using

laser spectroscopy to quantify extra-terrestrial atmospheric methane/ethane. This project encompasses a broad variety of habitats due to the dynamic nature of estuaries for comparative use in future studies to help determine biogenic versus thermogenic origins of light hydrocarbons.

This aims of this study are to:

- a) Quantify  $C_1$  and  $C_2$  concentrations along a temperate estuarine salinity gradient running from freshwater to marine through sediment cores, quantifying aqueous hydrocarbon concentrations using “purge and trap” apparatus and quantifying atmospheric concentrations
- b) Build an inventory of  $C_1/C_2$  ratios for future studies to use to contextualise astrobiological data.

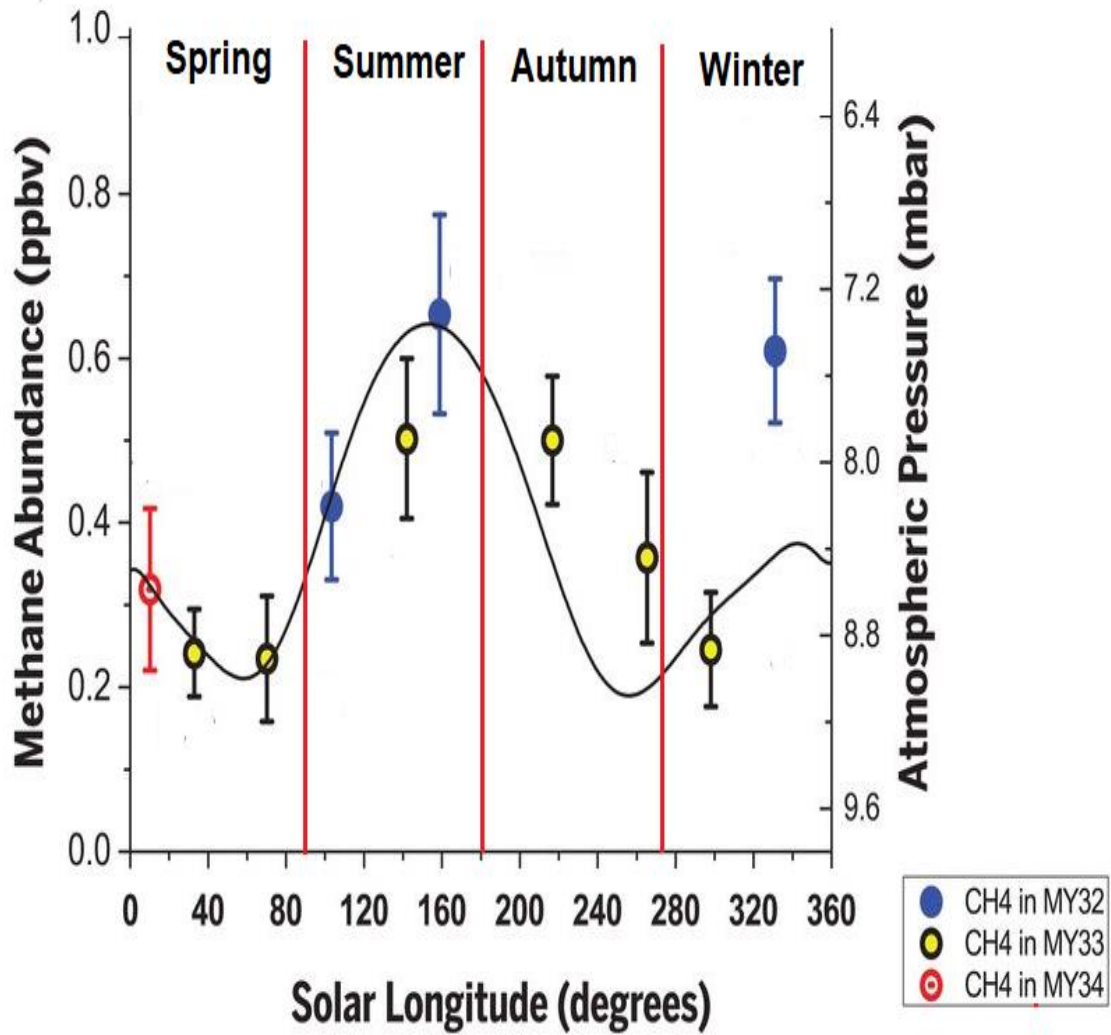


Figure 1.1: Seasonal variability in Martian background atmospheric methane at the Gale crater from the tunable laser spectrometer on the sample analysis at Mars instrument suite equipped on the Curiosity rover. MY = Martian year. All measurements are  $\pm 1$  S.E. Atmospheric pressure is represented by the solid black line and the inverted scale on the right for comparison. Adapted from Webster *et al.* (2018).

## Chapter 2 - Methods development

### 2.1 Introduction

Gas chromatography (GC) analysis is a robust, sensitive and reproducible method for the separation and quantification of gaseous samples and liquid solutions. Methane and ethane are gaseous by definition at most standard temperatures and pressures, falling under the umbrella of volatile organic compounds (VOCs) - carbon-containing compounds that have a high vapour pressure at standard room temperature (Steinke *et al.*, 2018). Gas chromatography with flame ionisation detection (GC-FID) is a principal analysis method for biogenic volatile alkanes/alkenes (Steinke *et al.*, 2018), which can be further coupled with purge-and-trap methodology for dissolved gas analysis. This study aims to quantify biogenic methane and ethane production along an estuarine gradient using *in-situ* analysis via flux chambers and tedlar bags and *ex-situ* using GC-FID with purge-and-trap apparatus and cavity ring-down spectroscopy (CRDS).

#### 2.1.1 Sampling strategy

Estuaries are a challenging environment for volatile analysis. Sedimentary production is a major source of methane (Oremland *et al.*, 1981; Hinrichs *et al.*, 2006; Xie *et al.*, 2013), particularly in estuarine waters, which emit 1.1 – 3.0 Tg CH<sub>4</sub> yr<sup>-1</sup> (Middelburg *et al.*, 2002). Estuaries link coastal marine systems with terrestrial aquatic systems, which are significant sources of methane to the atmosphere (Borges *et al.*, 2015), implicating estuaries in the emission of freshwater-derived CH<sub>4</sub>. Estuaries often exhibit high supersaturation of methane relative to the atmosphere (Middelburg *et al.*, 2002), due to both transport of freshwater-derived CH<sub>4</sub> and *in-situ* sedimentary methanogenesis. Dissolved ethane concentrations are many orders of magnitude lower than methane in most environments (Oremland *et al.*, 1981; Hinrichs *et al.*, 2006) therefore requiring sensitive analysis techniques.

Traditional gas chromatography with flame ionisation detection is useful for quantifying gas phase hydrocarbon emissions from gas-tightly sealed cultures, but cannot quantify dissolved gases without technical modifications. Purge-and-trap analysis (P&T) was used using a

purpose-built apparatus (Fig 2.1) connected to a Shimadzu GC-2014 (Milton Keynes, UK) which purges roughly 50 - 200 mL of an aqueous sample with an inert gas (typically N<sub>2</sub> or He) at a known flow rate (typically ~60 mL min<sup>-1</sup>), then drying the sample gas through use of a glass condenser (Fig. 2.1) submerged in ice water (or glass tubing filled with glass wool), followed by a Nafion counter-flow dryer (Permapure MD-050-72S-1, Lakewood, USA) before cryogenically enriching the dried analyte in a cryotrap suspended above (or in the case of helium purge gas, directly immersed into) liquid N<sub>2</sub>, sorbing the analyte to the trap. The analyte is then desorbed and flushed onto the column for analysis by immersing the trap in freshly boiled (>90 °C) water.

P&T methodology benefits from a superior sensitivity and flexibility compared to traditional direct injections. A vacuum pump installed into the system, pulling from the waste gas supply (Fig. 2.1) can transfer large volumes of analyte stored in a Tedlar bag onto the cryotrap, rather than piercing the septa to retrieve a small (200 µL) gas sample for direct injection and possibly compromising the sample. Headspace flushing of vials can easily be achieved by integrating an inflow and outflow port with needles to pierce septa of gas-tight vials (Fig. 2.1). This method also allows for qualitative retention time confirmation by injecting standard gases through the septum of a fresh vial and cryogenically enriching and then desorbing the analyte which is helpful for verifying gas compositions in environmental samples.

Franchini and Steinke (2016) compared sensitivities of P&T methodology versus direct gas phase headspace injections for the quantification of DMS, finding a sensitivity of 0.2 – 20 µM for direct headspace sampling, 50 – 250 nM for headspace purging of gaseous phase (Fig. 2.1) and sub-nanomolar range for in-tube purging of ~200 mL aqueous phase samples. Ethane and propane are found in trace concentrations in marine and estuarine water (see Chapter 1.5), favouring use of P&T methodology over traditional gas chromatography.

1

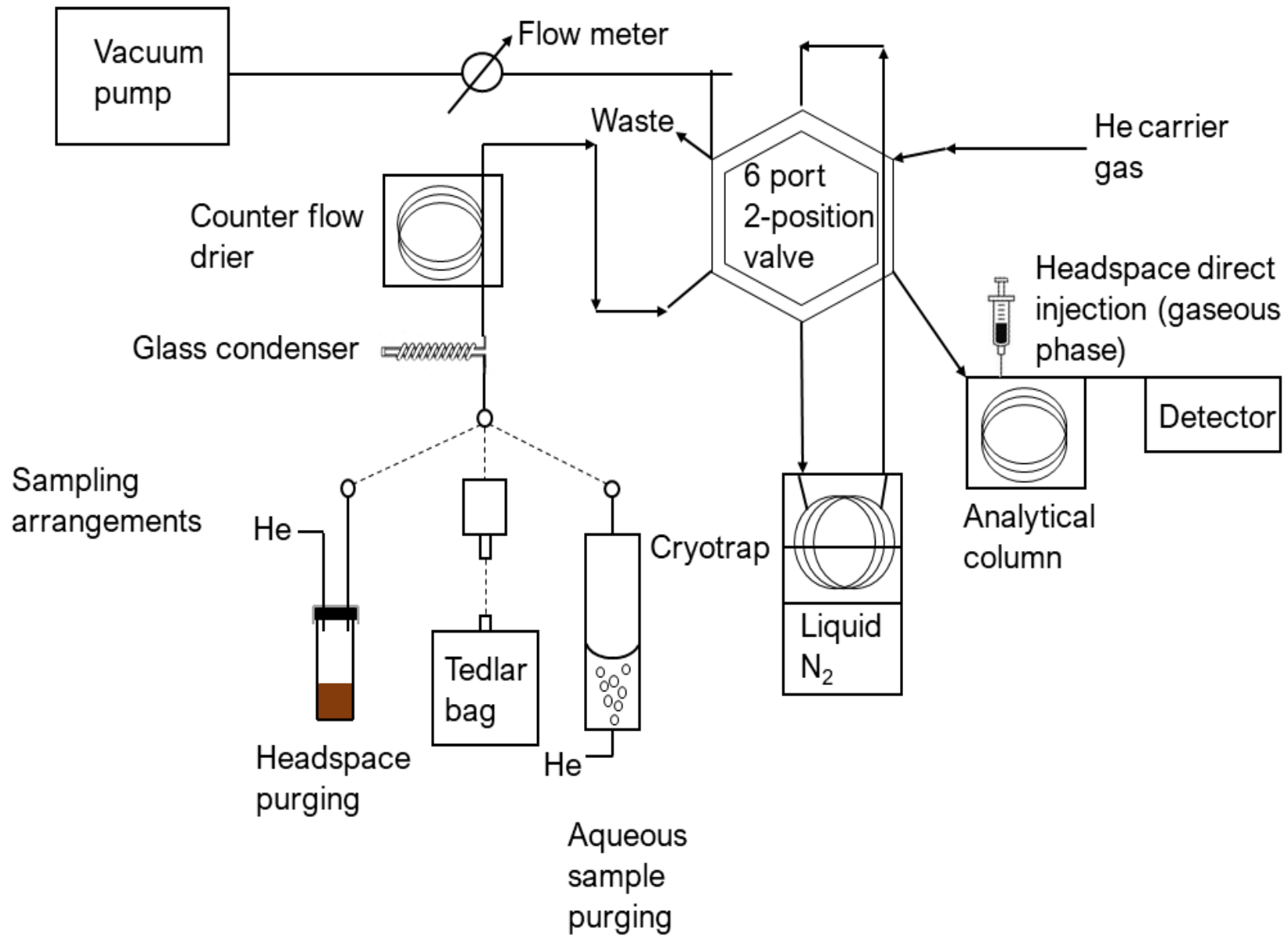


Figure 2.1: Schematic overview of the purge and trap system used for gaseous hydrocarbon analysis.

### 2.1.2 Real time spectroscopy for methane analyses

Real time analysis via portable spectrometers, particularly cavity ring-down spectroscopy (CRDS), is a relatively new method of analysing *in-situ* atmospheric gas concentrations. The CRDS (Picarro G4301a, Santa Clara, USA) uses a beam fired from a single-frequency laser diode entering a three-mirror cavity, then measures the exponential decay (“ring-down”) of residual light bouncing between the three mirrors within the empty cavity and compares this value to an accelerated ring-down time when a gas species is introduced ( $\text{CH}_4$ ,  $\text{CO}_2$  or  $\text{H}_2\text{O}$ ), producing precise, quantitative measurements accurate to parts per billion. The measurements produced are independent of laser intensity fluctuations and laser power, making them superior to traditional laser spectroscopy.

Methane fluxes in static chambers from soil-atmosphere exchange measured with CRDS captured 97% of fluxes in the field and 65% in the lab, while traditional chromatography only captured 16% of measured fluxes in the lab and none in the field, though comparisons for  $\text{CO}_2$  and  $\text{N}_2\text{O}$  revealed less of a difference between techniques (Oikawa, 2016). CRDS allows for more complete understanding of fluxes of atmospheric gases to the environment at both the sediment-air and water-air interfaces, while complementing data provided by more traditional techniques such as gas chromatography.

Traditional purge-and-trap chromatography did not cryogenically enrich methane in any of the calibration tests (see Appendix, Fig. A1), due to methane having a low boiling point ( $-161.5\text{ }^\circ\text{C}$ ) and a small molecular size. Therefore, this study expands CRDS technology to quantify dissolved methane using purpose-built apparatus (Fig. 2.2) for lab-based analyses of water samples. The sample is purged with inert nitrogen gas for 20 minutes at room temperature at  $60\text{ mL min}^{-1}$ , then passed through a small glass tube packed with glass wool and into a 5 L Tedlar™ bag. The bag is then attached to tubing connected to the CRDS, which vacuum pulls the sample from the bag through a glass purge tube filled with Drierite® desiccant pebbles and glass wool to further dry the sample, before finally passing into the CRDS through a particulate filter for analysis. Multiple drying steps are crucial, as any

moisture build up in the CRDS will eventually cause damage to the delicate systems and could affect the analyses. Environmental samples consistently had higher methane concentrations detected compared with a MilliQ™ water control, though a true negative control calibration using hydrocarbon-free water will be necessary for future verification (see Chapter 4.2 for suggestions).

## 2.2 Methods

### 2.2.1 *In-situ* flux analysis

*In-situ* deployable flux chambers in the field fitted with HOBO® light and temperature loggers (Fig. 2.3) are essential for capturing natural environmental flux data, which is necessary to build an understanding of the dynamic environment. *In-situ* gas chambers were constructed using 2 L clear polycarbonate bottles (Nalgene) with a diameter of 12.3 cm, and a polycarbonate lid. A sampling port made from a Swagelok 1/4" to 1/8" reducing union (Swagelok) containing a Polytetrafluoroethylene (PTFE) covered silicon septum (Sigma) was inserted to fit a Tedlar™ 5 L bag via Teflon 1/4" tubing for field samples (Fig. 2.3). The chambers were fitted with Swagelok blind ferrules when incubating samples which were removed and replaced with tubing after the incubation period was over.

Two chamber designs were implemented to capture the sediment-air and water-air interfaces (Figs. 2.4A and B). The water-air flux chambers (Fig. 2.3A) were kept afloat using polystyrene and anchored to shore using rope. After incubation for 5 minutes, the chambers were physically depressed 20 cm into the water, using positive pressure to force the sample gas into a Tedlar™ bag which was then stored in the dark. Initial incubations were for 10 minutes but reduced to 5 minutes to avoid condensation and increasing heat issues. The sediment-air chambers (Fig. 2.3B) were deployed for 5 minutes, then connected to a vacuum pump via a 1/4" Swagelok union connector. These chambers were fitted with another connection to a second Tedlar™ bag containing 1 L N<sub>2</sub>, which prevents the following vacuum pumping step from forcefully sucking in indigenous gases sorbed to the sediment, which could artificially inflate the flux calculations. The gaseous flux sample was vacuum

pulled at  $1 \text{ L min}^{-1}$  for 4 minutes into an empty Tedlar™ bag, then stored in the dark until further analyses. Triplicate chambers were deployed in the field for each air interface and site.

Flux calculations for the sediment chambers assumed instant mixing in the chamber, which could be achieved in future studies by integrating a fan in the chambers. A quadratic model of time against cumulative sample % in the sample Tedlar™ bag was created and analysed for statistical significance and the corresponding  $R^2$  value.

### *2.2.2 Physical measurements*

Field measurements were broadly divided into atmospheric, sediment and water samples, each requiring some methods development to streamline collection and laboratory protocols. Atmospheric samples were collected initially using a 100 mL plastic disposable syringe (Fisher, UK) and a T (3-way) stopcock (Vygon, Swindon, UK) connected to a 5 L Tedlar™ bag and a small (~30 cm long) piece of tubing. 1 L air samples were collected by sucking in 100 mL of air, then rotating the stopcock to store the sample in the Tedlar™ bag, then repeating 9 more times. This method was effective for small volumes of air but required tracking how many times the syringe had been pumped, leading to frequent human error. This method was then replaced with a vacuum pump (Sigma, UK) and a 1 m length of PTFE tubing, allowing for more accurate sample collection.

Sediment was initially collected in triplicate 10 cm diameter cores to 5 cm depth from Hythe in January 2019 (Fig. 3.1) as a trial “proof of concept” pilot study. The sediment was stored in a cool box and brought back to the lab, where it was mixed 1:1 by volume with estuarine water from Hythe. 15 mL of sediment slurry was then pipetted into 27 42 mL sterile glass vials (Fisher, UK) and gas-tightly crimp sealed with sterile butyl rubber stoppers. 9 vials were left as unamended slurry, with a further 9 receiving a 210  $\mu\text{L}$  addition of 2-BES to observe methanogenic inhibition. The last 9 vials were covered with foil and autoclaved at  $120 \text{ }^\circ\text{C}$  before sealing the vials as above, to create abiotic control conditions. All vial headspaces were then flushed with a 4:1 mixture of  $\text{H}_2:\text{CO}_2$  for two minutes at  $60 \text{ mL min}^{-1}$  to create

anoxic conditions favourable for methanogenesis. The vials were stored in the dark at room temperature until analysis.

Initial measurements were confounded due to the rubber stoppers being too thick for standard gas-tight syringes to pierce without bending the needle. A variety of syringes/needles were tried, including disposable sterile BD microlances (orange 16mm x 0.25 gauge, Fisher) and a Luer twist fit with gas-tight valve. The most effective and simple method was found to be using a standard needle and gently guiding the needle through the stopper, taking care to clean the needle of any stray rubber using a thin metal wire between samples and checking the syringe is not blocked by observing air bubbles coming out of the needle when lab air is pushed through a MilliQ water vial.

Triplicate 100 mL water samples were collected using clean 100 mL glass syringes with a Luer connection to ¼" Teflon™ tubing with double T (3-way) stopcock (Vygon, Swindon, UK). The valves allow the tubing to flood with sample water, enabling a bubble-free water sample. Temperature and pH of the estuarine water was measured using a calibrated multiprobe. Triplicate atmospheric samples were collected by vacuum sucking 5 L of air at 1 L min<sup>-1</sup> at each site during low tide then stored in gas bags in the dark.

1

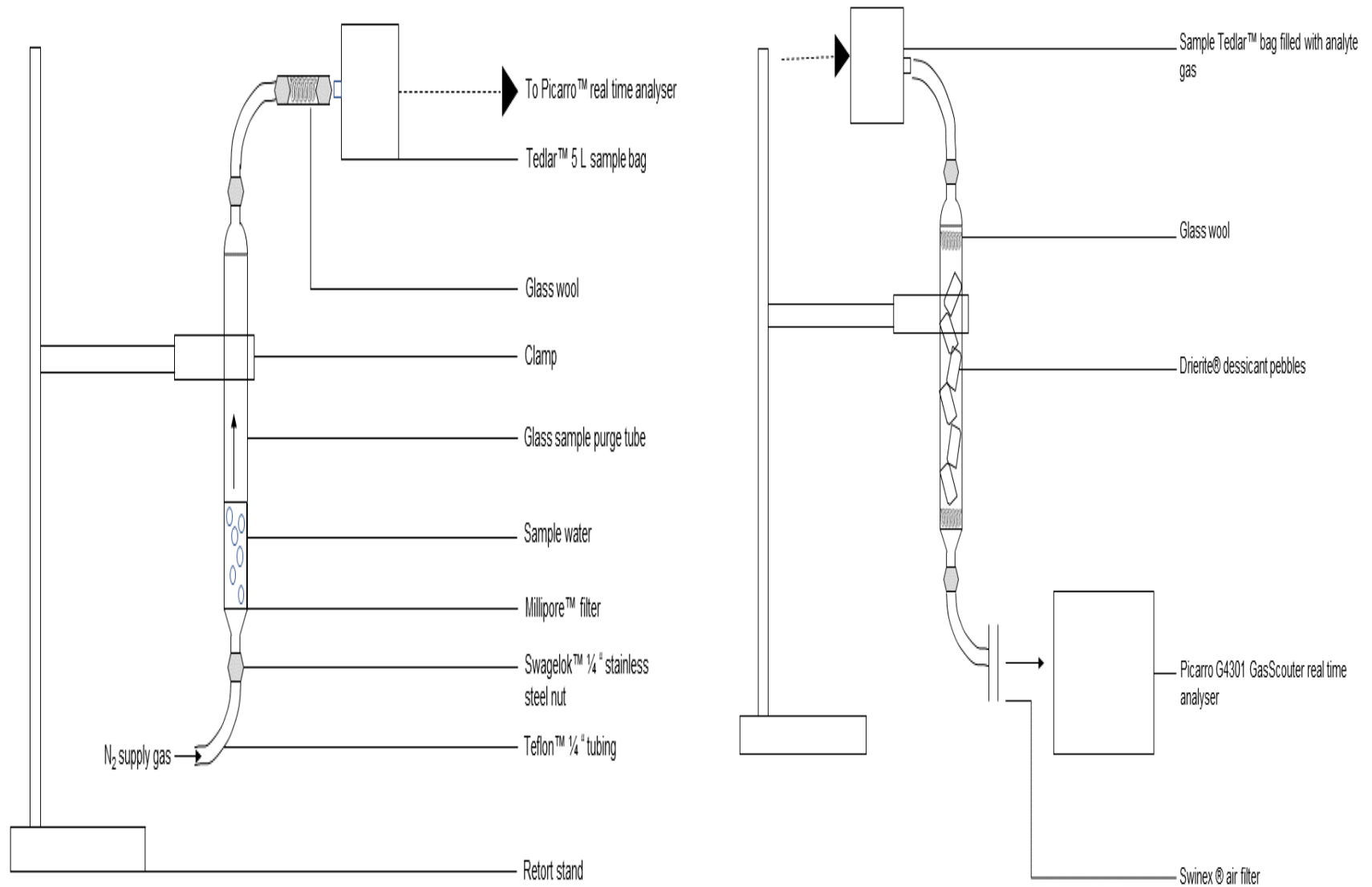


Figure 2.2: Purpose-built aqueous methane purging apparatus. The dotted arrow represents physically removing the Tedlar™ 5 L bag from the initial apparatus (a) and reattaching it to the secondary apparatus (b).

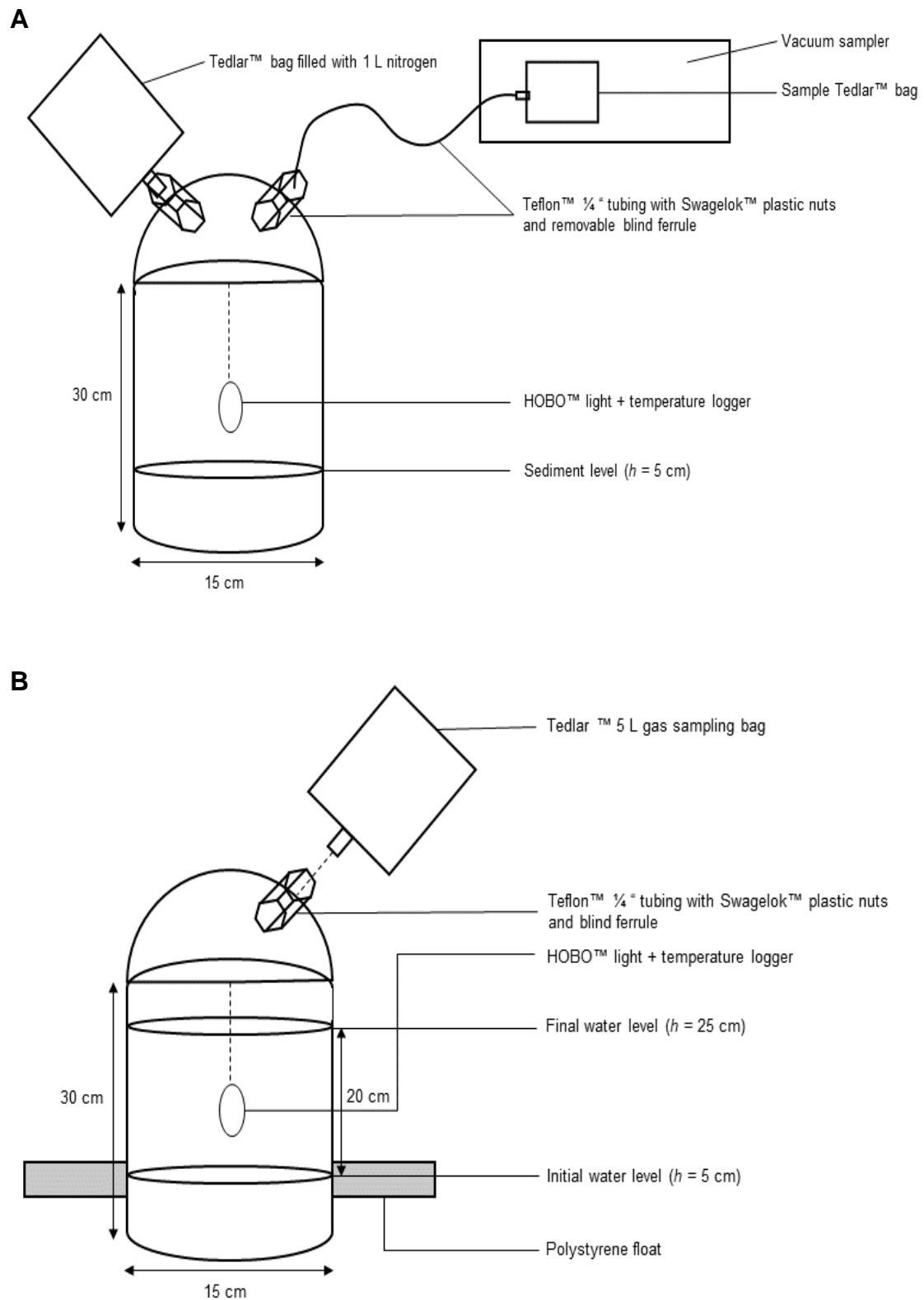


Figure 2.3: Purpose built flux chambers for *in-situ* gaseous flux analysis. **A** – Flux chamber design for the sediment-air interface; **B** – Design for the water-air interface.

### 2.2.3 Calibrations

Gaseous hydrocarbon quantification spread across aqueous, atmospheric and emissions from sediment cultures required various calibrations.

The CRDS was calibrated using 5 L Tedlar bags filled with 3 L of inert N<sub>2</sub> (BOC, UK) and methane concentrations varying from 0 – 2 ppm. Samples were dried using a Restek moisture trap (PN: 22014, Restek, UK) connected to 1/8" Teflon tubing and a 25 mm Swinnex™ (Fisher Scientific, Loughborough, UK) air filter to remove particulate contamination before entering the instrument for analysis. The instrument readings on the analyser GUI were allowed to stabilise (~ 2 mins) after connecting to the tedlar bag, before noting the average CH<sub>4</sub> concentration across 1 minute in ppm (Fig. 2.5).

A GC (Model 2014; Shimadzu, Milton Keynes, United Kingdom) equipped with a capillary column (50 m × 0.53 mm × 10 µm Rt-Alumina BOND/KCl; Restek, Saunderton, United Kingdom) and a flame-ionization detector was used for headspace hydrocarbon determination. Initial methodology used an oven temperature ramp from 40 °C for 5 minutes to 180 °C at 10 °C min<sup>-1</sup> for a total run time of 35 minutes, though an isothermal method at 40°C for 5 minutes was later found to be ideal for light hydrocarbon quantification (see Appendix, Table A1). 1000 ppm standard gas bottles of methane, ethane and propane (Calgaz, Newcastle, United Kingdom) were used for calibrations. 0 – 150 µL samples were taken from the CH<sub>4</sub> standard and directly injected into the GC using a gas-tight syringe (SGE, Milton Keynes, United Kingdom). The linear relationship between peak area and injected moles of methane was then calculated, giving a final calibration curve (Fig. 2.6). A similar process was used for ethane and propane, though smaller volumes were used (0 – 6 µL) to reflect the lower natural concentrations of these gases (Fig. 2.6).

Calibrating the purge and trap apparatus took multiple steps to reach a satisfactory calibration for ethane and propane. Initial calibrations used a purpose-built P&T system using 1/16" stainless-steel tubing (Restek, Saunderton, United Kingdom) with stainless steel Swagelok™ connections, a 3 m stainless steel cryotrap and a liquid N<sub>2</sub> boiler (Fig. 2.1) to

keep the cryotrap at 150 °C during cryogenic enrichment, with N<sub>2</sub> as the purge gas. Calibration standards were prepared using 5 L Tedlar™ bags (Supelco, Sigma-Aldrich, Dorset, UK) filled with 3 L of N<sub>2</sub> gas and varying concentrations of methane, ethane and propane at 0 – 2 ppm CH<sub>4</sub> / 0 - 2 ppb C<sub>2</sub>H<sub>6</sub>/C<sub>3</sub>H<sub>8</sub>, respectively. Samples were sucked through the P&T system via a vacuum pump (Fig. 2.1) for 10 minutes at 60 mL min<sup>-1</sup>, before flushing the analyte into the GC. However, a satisfactory calibration was not achieved using this method, nor via changing the temperature of the cryotrap. Methane was found to not cryogenically enrich, whereas ethane non-linearly responded to the calibration (see Appendix, Fig. A2). A glass lined, stainless-steel based P&T system (Fig. 2.1) was then used for all further analysis, and the purge gas was switched to helium to allow complete immersion of the cryotrap in liquid nitrogen, removing the need for temperature control of the trap. Calibrations were reconducted using the same method, with results summarised in figure 2.7.

#### *2.2.4 Statistical analysis*

Calibration curves and R<sup>2</sup> values were created in Excel (Microsoft Office 365 ProPlus). All other statistics were created in Rstudio version 1.0.153 using R version 3.5.2 (2018-12-20) - "Eggshell Igloo". Sediment treatment conditions effect on CH<sub>4</sub> production were statistically tested using a one-way ANOVA with a post-hoc Tukey's HSD test.

#### *2.3 Results*

Calibration of the CRDS revealed a good linear regression (R<sup>2</sup> = 0.95) between 0 – 2 ppm CH<sub>4</sub>. Strong linear regressions (R<sup>2</sup> > 0.97) were found for both direct injections (Fig. 2.6) and P&T (Fig. 2.7) methodology, though CH<sub>4</sub> was not cryogenically enriched using P&T methodology. Methane eluted after ~1.5 mins, with ethane following at ~1.7 mins and propane at ~3.6 mins.

Sediment incubations revealed methanogenic activity (Fig. 2.8). Unamended vials had a mean concentration ± standard deviation of headspace CH<sub>4</sub> of 4250.10 ± 2071.74 nmol CH<sub>4</sub>, while inhibited vials showed a mean value of 33.11 ± 28.77 nmol CH<sub>4</sub> and controls had 7.88

$\pm 0.04$  nmol CH<sub>4</sub>. Unamended vials produced significantly more methane than inhibited and control vials ( $F_{(2, 24)} = 4.168$ ,  $p < 0.05$ ) and post-hoc analysis revealed no significant difference in methane concentration between inhibited and control vials ( $p > 0.05$ ).

No ethane or propane were found in water samples collected from the river, though ethane was found in atmospheric samples (peak area = 1762.5 – 4512.4).

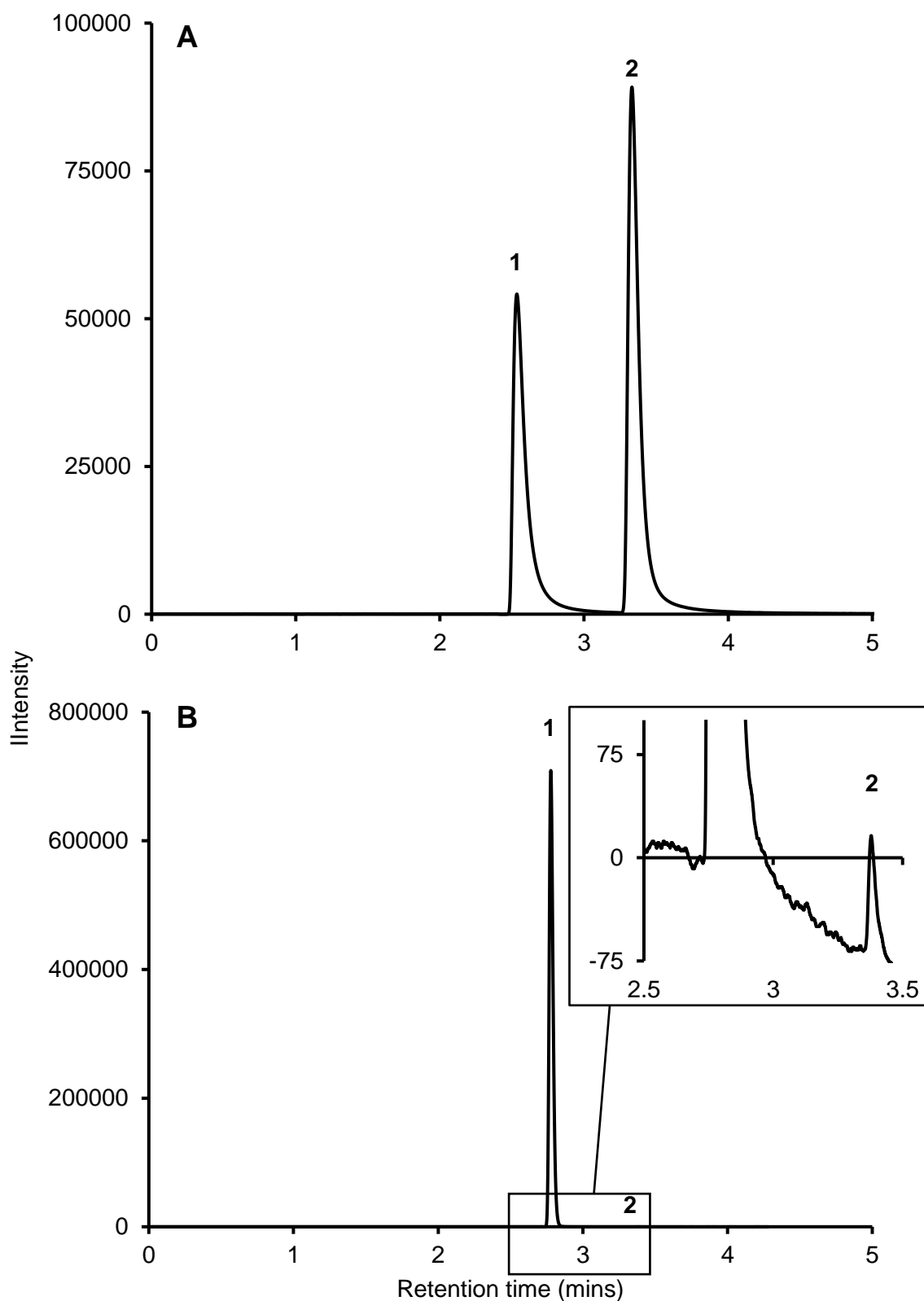


Figure 2.4: Representative chromatograms for methane (1) and ethane (2). **A** - Calibration chromatogram using standard gases (BOC, >99% sample); **B** - Environmental sample, collected from the headspace of a sediment slurry incubation.

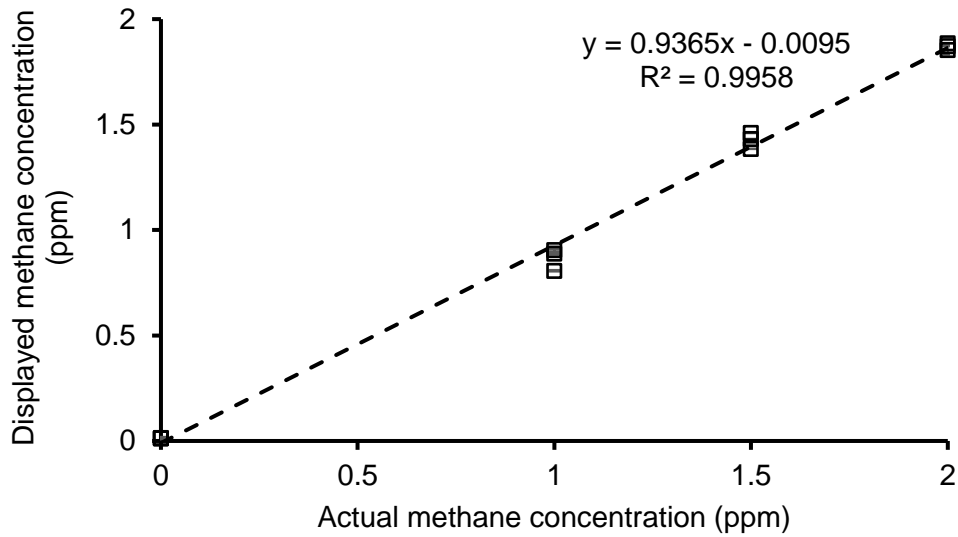


Figure 2.5: Linear regression for calibrating the CRDS (Picarro G4301a GasScouter), prepared using Tedlar™ 5 L bags ( $n = 12$ ) filled with 3 L  $N_2$  and 0 – 2 ppm  $CH_4$  from a standard gas bottle (BOC, UK).

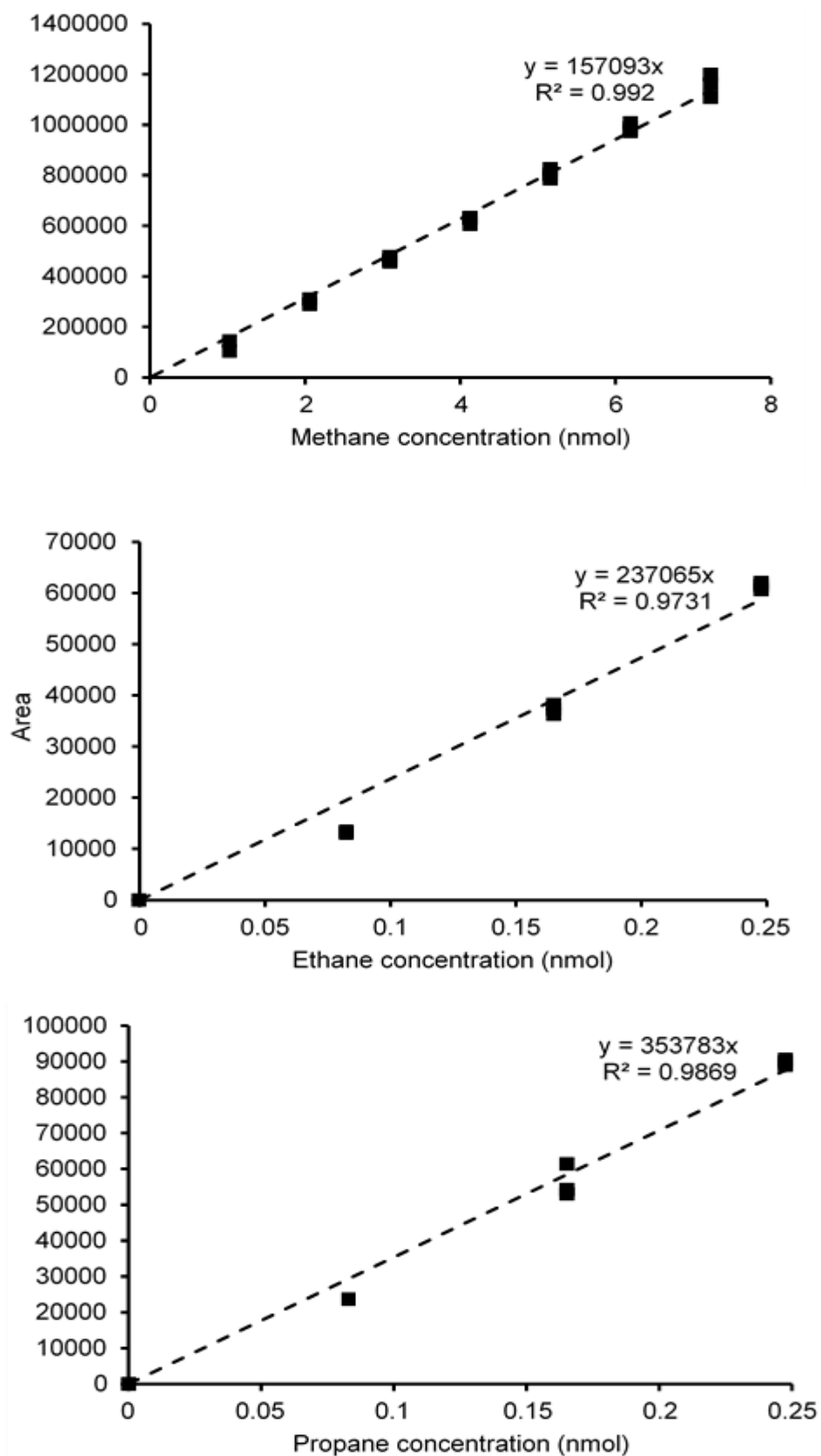


Figure 2.6: Linear regressions for methane (top), ethane (middle) and propane (bottom), prepared using 0 – 150  $\mu\text{L}$   $\text{CH}_4$  and 0 – 6  $\mu\text{L}$  ethane and propane from standard gas bottles (BOC, UK), injected directly into a GC-FID (Shimadzu, Milton Keynes, UK).

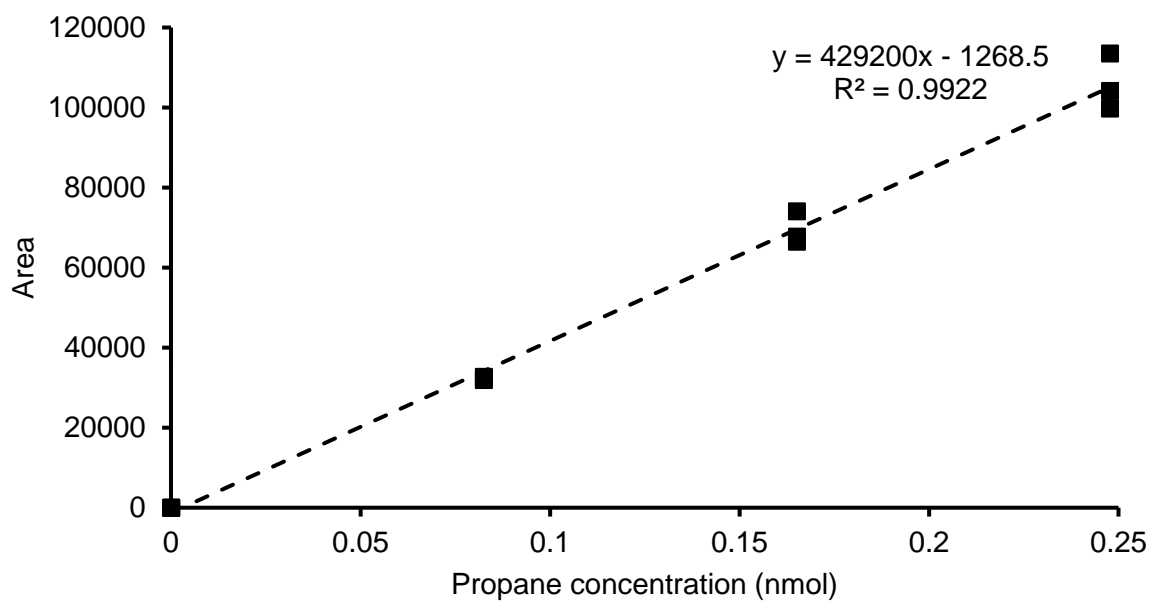
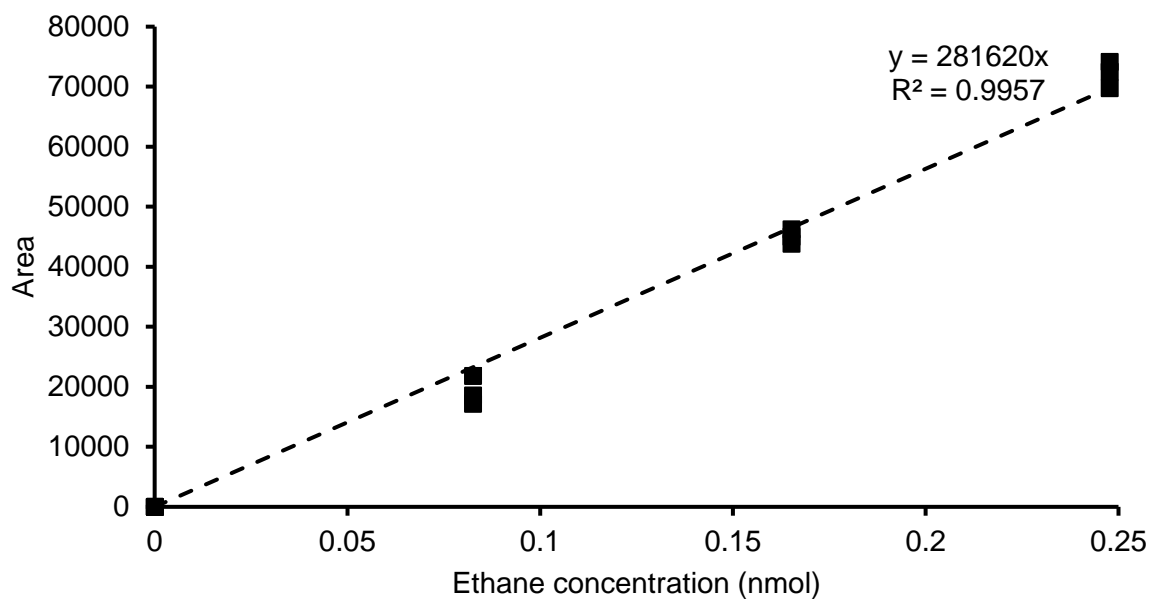


Figure 2.7: Calibration curves created using 0 – 6  $\mu\text{L}$  of 1000 ppm ethane/propane standards in 3 L Tedlar™ bags, vacuum sucked through a glass lined P&T system for 10 minutes at  $60 \text{ mL min}^{-1}$  before desorption via immersing the cryotrap in freshly boiled water ( $>90 \text{ }^\circ\text{C}$ ) and flushing the analyte into a Shimadzu GC-2014 equipped with FID.

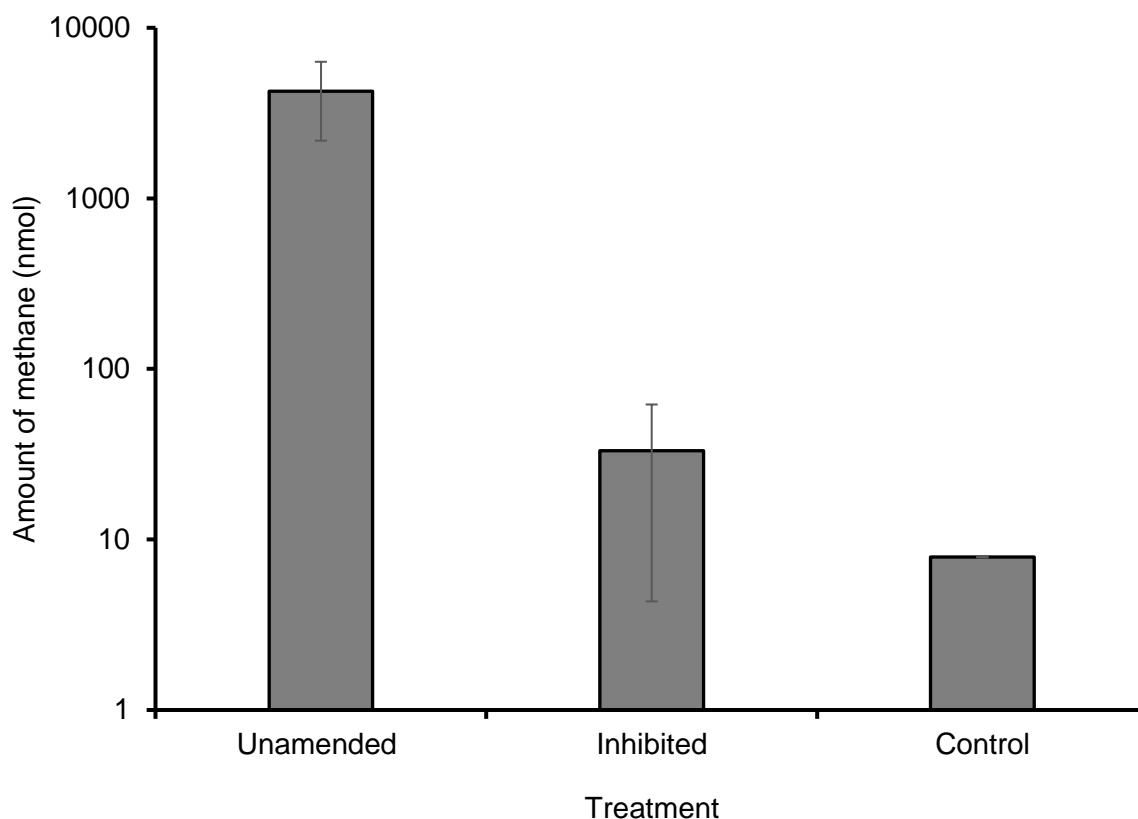


Figure 2.8: Production of methane in gas tight sediment cultures collected from the River Colne, Hythe, UK, incubated for >30 days. Treatment conditions are unamended (headspace flushed with 4:1 H<sub>2</sub>:CO<sub>2</sub>), inhibited (addition of 0.007 M 2-BES) and control (autoclaved at 120 °C). Note that data are presented along a log<sub>10</sub> scale for clarity. All values are ± s.e. (n = 27)

## 2.5 Discussion

The calibrations provided high linear regression coefficients that were used to convert peak areas into concentrations of methane, though also revealed methane cannot be cryogenically enriched using available P&T methods. Broadgate *et al.* (1997) used a glass-bead packed cryotrap to quantitatively concentrate methane, which increases the surface area for CH<sub>4</sub> to sorb onto the cryotrap. Donval and Guyader (2017) used an alternate “headspace” method to determine methane and nitrogen concentrations in 300 mL seawater samples, whereby seawater is allowed to come to equilibrium in a gas-tightly closed syringe, followed by headspace sampling and injection into a GC. The study found good linear regressions of CH<sub>4</sub> and N<sub>2</sub> via this method against traditional purge-and-trap

chromatography, suggesting the headspace method is a viable alternative to purge-and-trap chromatography for methane analysis. These studies confirm the observations that methane is unable to cryogenically enrich on a purge-and-trap apparatus without specific, sensitive adjustments.

The methane purging apparatus connected to the CRDS described in section 2.1.2 was tested via comparing MilliQ water controls ( $n = 3$ ) to environmental samples ( $n = 9$ ), finding a range of 0 – 0.064 ppm CH<sub>4</sub> in control samples and 0.027 – 0.101 ppm CH<sub>4</sub> in environmental samples. These ranges mostly did not overlap and so the control values were subtracted from environmental values for the results in chapter 3. This verification method was efficient but the controls were not hydrocarbon-free, which could be achieved by using ultra-high purity water in future studies.

Methane concentrations in the headspace of sediment cultures overshadowed other trace gases, including ethane and propane. These methods developments shows P&T analysis could be used to determine the concentrations of these trace gases, as methane is not cryogenically enriched and therefore cannot overshadow other VOC's.

*In-situ* quantification of methane and ethane emissions using purpose-built flux chambers (Fig. 2.4) had multiple design considerations. The designs for the chambers in this study benefit from their simplicity, ease of use and portability. Eklund (1992) suggest that flux chambers with low height-to-width ratios, such as square/rectangular shapes, are inefficient due to potentially inadequate mixing of the interior chamber atmosphere. However, Adams *et al.* (1980) compared flux chamber geometry between 11 designs, choosing a cylindrical design with a flat top, similar to this study's chamber designs (Fig. 2.4). Furthermore, vertical and horizontal composition profiles were performed with no stratification detected, refuting concerns mentioned earlier from Eklund (1992). Eklund (1992) compared their dome shaped flux chamber to the cylindrical design from Adams *et al.* (1980) under field conditions and found no statistically significant differences in gas concentrations, further demonstrating cylindrical flux chambers as effective. However, the sediment chamber design used in this

study assumes instant mixing in the sample concentration calculations, which may lead to significant errors across a large-scale deployment in future studies – therefore, a design more akin to Eklund (1992) may be more suitable in this scenario.

Methane production in unamended sediment vials compared to inhibited and control vials clearly demonstrate methanogenic activity in Hythe sediments. The methane production was orders of magnitude larger in the unamended vials (Fig. 2.7), confirming this as an effective method of *ex-situ* methane quantification from sediments. Production rates can be obtained by measuring every 24 hours, and potentially could allow for pure culture obtainment and genetic sequencing for a complete understanding of methanogenesis in a given area. The ease of set-up of this analysis facilitates larger scale studies and can be used as a blueprint for further research in this area.

## Chapter 3 – Methanogenesis in a temperate estuary

### 3.1 Introduction

Estuaries are semi-enclosed, dynamic bodies of water that provide an interface between riverine and marine habitats. Steep physico-chemical gradients are common in estuaries, varying based on geomorphology and tidal heights (Bernhard and Bollmann, 2010).

Dissolved nutrient and ion concentrations often follow gradients of decreasing concentrations from the freshwater head of the estuary to the mouth (e.g. nitrogen) or vice-versa (sulphate, sodium) (Nedwell *et al.*, 2016).

The River Colne is a freshwater river that flows into and produces the Colne/Blackwater estuary complex, located in Essex, UK, typical of the muddy estuaries in the east of England. The Colne estuary is considered a model habitat for estuarine research and has been referred to as “a microbial observatory” (Nedwell *et al.*, 2016). The estuary has been the focus of research efforts, particularly at the University of Essex, for over 40 years, leading to it being one of the most intensively studied temperate estuaries in the northern hemisphere (Nedwell *et al.*, 2016). The Colne estuary is a turbid, hypereutrophic mesotidal estuary with a depth range of 1.5 m to >15 m from the head to the mouth of the estuary respectively (tidal amplitude of around 4 m). Salt marshes line over 900 ha of the channel, with creeks draining into the main estuary channel. A large sewage treatment works (STW) is located near the head of the estuary, as well as several smaller STW facilities along the course of the estuary, servicing much of Colchester with its 194,706 strong population. This contributes strongly to the estuarine hypereutrophication, resulting in levels as high as 1 mM nitrate and 50  $\mu$ M phosphate near the main STW outflow (McMellor and Underwood, 2014). Turbidity reaches a maximum towards the middle, brackish waters of the Colne estuary halogradient (~15 – 30 ‰ salinity), which coupled with several nutrient gradients (Table 3.1) influences the composition of microbial communities present in the estuary in the sediment and water column. Estuaries often exhibit heightened levels of organic matter and nutrients relative to other bodies of water, which results in elevated primary production and

heterotrophic activity, facilitating a complex microbial community in the upper sediment (~2 cm depth). Tight metabolic and substrate coupling between diverse phylogenetic groups and abundance of narrow functional niches allow for a wide range of microbial organisms to reside in the estuarine sediments (Wolanski and Elliott, 2016). These hydrogeological and physico-chemical features make the River Colne a representative example of many northern hemisphere estuaries and an excellent model habitat for microbial research (Nedwell *et al.*, 2016).

### 3.1.1 Methanogenesis in the River Colne

Estuarine methanogenesis alongside sulphate reduction in the River Colne are major terminal steps in carbon cycling. Archaeal communities consisting of Euryarchaeota, Bathyarchaeota and many other phyla vary in relative proportions through the course of the estuary (Webster *et al.*, 2015). A metagenomic analysis of the estuary demonstrated that members of the Bathyarchaeota were the most commonly found archaea, representing 41% of 16S rRNA gene libraries by PCR cloning (Webster *et al.*, 2015). The low salinity Hythe sediments are dominated by acetotrophic *Methanosaeta* and putatively hydrogenotrophic *Methanomicrobiales* whilst the high salinity Brightlingsea site was characterised by *mcrA* genes attributed to methylotrophic *Methanococcoides*, *Methanosarcina* and the methanotrophic ANME-2a group (Webster *et al.*, 2015). Sulphate reduction in the Colne estuary sediments was measured to be two orders of magnitude greater than methanogenesis, even in the upper estuarine sediments where there is lower available sulphate (Nedwell *et al.*, 2004). Hythe sediments had  $51.7 \pm 5.1 \text{ mmol m}^{-2} \text{ a}^{-1} \text{ CH}_4$  formation with around half of this reaching the atmosphere ( $22.3 \pm 0.6 \text{ mmol m}^{-2} \text{ a}^{-1} \text{ CH}_4$ ), representing a significantly active methanotrophic population (Nedwell *et al.*, 2004). The active methanogenic community in the Colne estuary sediments make it an ideal habitat for exploring methane production across a salinity gradient, as well as investigating ethane dynamics, which has not been done in the Colne estuary before.

### 3.1.2 Research aims and hypotheses

This research aims to develop understanding of methane and ethane emissions from a temperate estuary, through sediment incubations, dissolved gases in the water column analysis and *in-situ* flux analysis.

#### *Hypotheses:*

- a) Dissolved methane and ethane concentrations from estuarine water samples will be significantly different between the sampling sites.
- b) *Ex-situ* sediment incubations will have significantly more methane and ethane produced in unamended vials compared to inhibited and control vials.
- c) *Ex-situ* sediment incubations will differ significantly in headspace methane and ethane concentrations between sampling sites.
- d) Methane and ethane fluxes at both the sediment – air and water – air interfaces will be significantly different between sampling sites.

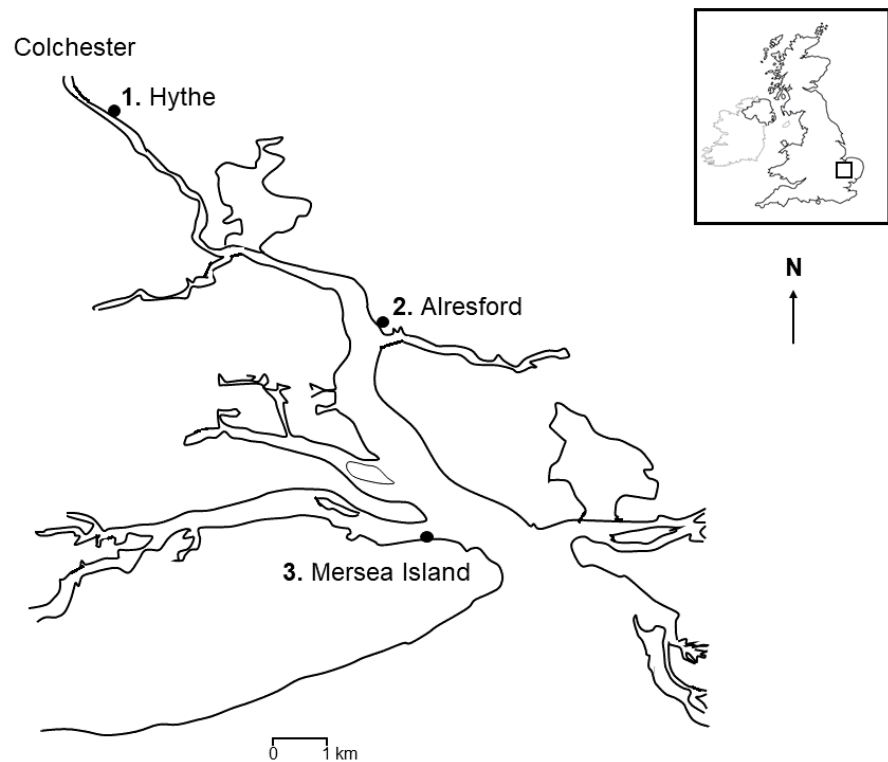


Figure 3.1: Locations of the three sampling sites along the River Colne, Essex. Sites are 1. Hythe, a mud flat at the estuary head; 2. Alresford, a mid-estuary creek and 3. Mersea Island, a brackish – mostly marine habitat at the estuary mouth.

## 3.2 Methods

### 3.2.1 Field Sampling

Sampling took place along the River Colne estuary in Colchester, Essex (Fig. 3.1) in September 2019. Sample sites were Hythe, a mud flat at the estuary head ( $51^{\circ}52.687' \text{ N}$ ,  $00^{\circ}56.011' \text{ E}$ ), Alresford, a mid-estuary creek ( $51^{\circ}50.716' \text{ N}$ ,  $00^{\circ}58.912' \text{ E}$ ) and Mersea Island, a brackish habitat located near the estuary mouth ( $51^{\circ}48'13.55'' \text{ N}$ ,  $0^{\circ}59'24.88'' \text{ E}$ ). The distance between the Hythe and Mersea Island sites is 6.16 km and follows the estuarine salinity gradient. Field sampling was conducted at low tide while estuarine water was collected at high tide of the same day. Conductivity and pH of the estuarine water were

measured in triplicate using a calibrated multiprobe. Conductivity ( $\text{mS cm}^{-1}$ ) was then converted to salinity (ppt) (Table 3.2).

### *3.2.2 Sediment incubations*

Sediment cores (10 cm diameter) ( $n = 3$ ) were collected at low tide from each site, then sieved through 0.2 mm sediment filters and mixed 1:1 by volume with estuarine water from their respective sites. Slurry mixtures of 10 mL were aseptically pipetted in a class 2 microbiology safety cabinet into 42 mL sterile glass vials (Fisher, UK). The vials ( $n = 9$ ) were then crimp sealed immediately with butyl rubber stoppers for unamended sediment vials ( $n = 9$ ). An addition of 210  $\mu\text{L}$  of the methanogenic inhibitor 2-bromoethanosulfonic acid (2-BES) (Merck, UK) made a final concentration of 7 mM in the inhibited vials ( $n = 9$ ), while the control slurries ( $n = 9$ ) were capped with aluminium foil and autoclaved at 120 °C to halt biological activity, then gas-tightly sealed. The headspace of all vials (unamended, inhibited and controls) were flushed using a 4:1 mixture of  $\text{H}_2:\text{CO}_2$  (BOC, UK) for 5 minutes to create a favourable environment for hydrogenotrophic methanogenesis and to remove any hydrocarbons in the headspace. The vials were incubated for a period of 44 days in the dark at room temperature and measured multiple times weekly using 50  $\mu\text{L}$  manual headspace injections into a GC-FID (as described in chapter 2.2.2).

### *3.2.3 Sediment water and organic content*

Sediment collected for organic carbon content analysis was transferred to sterile plastic plates and weighed, then dried in an oven at 60 °C overnight for gravimetric water content analysis. The dried sediment was transferred to crucibles and placed into a muffle furnace for 5 hours to burn off organic matter and weighed again for ash-free dry weight calculations.

### *3.2.4 Trace gas analysis in water and atmospheric samples*

Water samples for purge-and-trap analysis were collected bubble-free using methodology described in chapter 2.2. Bubble-free water samples were kept chilled in a cool box during transport from the field to the lab. The syringes containing the water samples were gradually brought to room temperature, before 50 mL was passed into a glass purge tube (Fig. 2.1)

through a 25 mm diameter, 0.6  $\mu\text{m}$  pore size Whatman GF/F filter (Fisher, UK). Gases were stripped from the aqueous sample by bubbling inert helium through the sample estuarine water at 60 mL  $\text{min}^{-1}$  for 20 minutes, allowing dissolved hydrocarbons ample time to cryogenically enrich on the cryogenic loop immersed in liquid  $\text{N}_2$  (see chapter 2.2 for further details on cryogenic enrichment of sample gases). All bubble-free water samples were measured on the same day of collection.

Atmospheric samples were collected in triplicate in Tedlar™ bags by vacuum sucking air at 1 L  $\text{min}^{-1}$  for 3 minutes from each site. Flux chambers (Fig. 2.3) were deployed in triplicate for both the sediment – air and water – air interfaces for 5 minutes at each site. Atmospheric samples were used to correct trace gas concentrations in flux-chamber samples when calculating flux values for each site.

### 3.2.5 Dissolved nutrient determination in estuarine water samples

Estuarine water for nutrient analysis was passed through 25 mm diameter 0.6  $\mu\text{m}$  pore size Whatman GF/F paper filter into sterile plastic universals then kept frozen at  $-5\text{ }^\circ\text{C}$  until analysis. Samples were analysed using a dissolved nutrient autoanalyzer (SEAL analytical, UK), targeting nitrite ( $\text{NO}_2^-$ ), phosphate ( $\text{PO}_4^{3-}$ ), nitrite ( $\text{NO}_3^-$ ), silica (Si) and ammonium ( $\text{NH}_4^+$ ).

### 3.2.6 Statistical analysis

Graphical representations and general data management were carried out in Excel (Microsoft Office 365 ProPlus). Statistical analyses were created in Rstudio version 1.0.153 using R version 3.5.2 (2018-12-20) - "Eggshell Igloo". All ANOVA models were post-hoc analysed using Tukey's HSD test. Dissolved hydrocarbon ( $\text{CH}_4$  and  $\text{C}_2\text{H}_6$ ) concentrations, dissolved nutrient concentrations, pH and conductivity variation across sites were analysed using one-way ANOVAs. Organic content in sediments was analysed using a chi-square test of goodness of fit. Trace gas concentrations in flux-chamber samples were analysed using a two-way ANOVA model, factored by study site and interface type (sediment-air or water-air). Sedimentary  $\text{CH}_4$  emissions from *ex-situ* gas-tightly sealed

sediment slurries were analysed using a two-way ANOVA, factored by treatments (unamended, inhibited and control samples) and by study site. Sedimentary C<sub>2</sub>H<sub>6</sub> emissions from *ex-situ* incubations were analysed using a three-way ANOVA model, factored by treatments, study site and incubation time, which was defined as “early incubation period” (<20 days) and “late incubation period” (>20 days). This was done to statistically determine if ethane was increasing in concentration over the course of the incubation period across all samples.

Dissolved nutrients were correlated with dissolved hydrocarbon concentrations in estuarine water samples using Pearson’s product-moment correlation. C<sub>1</sub>/C<sub>2</sub> ratios in dissolved estuarine water samples and flux measurements were calculated using average values for methane and ethane, in picomolar (pM). *Ex-situ* sediment slurry ratios were calculated by taking the final values for headspace methane and ethane on day 43 of incubation. Ratios from measurements from water samples were statistically analysed using a one-way ANOVA, factored by study site. Ratios from flux measurements were analysed using a two-way ANOVA, factored by study site and flux type (sediment – air or water – air interfaces).

### 3.3 Results

#### 3.3.1 General physico-chemical characteristics of the Colne Estuary

General diagnostic measurements of the Colne Estuary are summarised in tables 3.1 and 3.2. Salinity (derived from conductivity) followed a steep gradient from the head of the estuary at Hythe ( $16.47 \pm 0.586$  ppt) to the mouth at Mersea ( $40.90 \pm 0.100$  ppt).

Conductivity was found to significantly differ across all sites ( $F_{(2,6)} = 9829$ ,  $p < 0.01$ ,  $n = 9$ ).

Comparatively, pH was fairly consistent, with a range of 0.1 between the lowest pH at Alresford ( $9.49 \pm 0.050$ ) and the highest at Mersea ( $9.59 \pm 0.045$ ), and did not significantly differ between sites ( $F_{(2,6)} = 4.215$ ,  $p > 0.05$ ,  $n = 9$ ). Sediment collected from Hythe were driest with a 60.58% water content, whereas Alresford sediment had 72.26% and Mersea sediment had the highest water content at 95.02% (all samples  $n = 1$ ). Organic content did not differ significantly between sites ( $\chi^2_{(2)} = 4.11$ ,  $p > 0.05$ ,  $n = 9$ ).

Dissolved nutrients from estuarine water samples (Table 3.1) were highest in Hythe except for ammonium, which was highest at Alresford. A clear trend from highest dissolved nutrient concentrations at the head of the estuary to the lowest concentrations at the mouth is observable for all nutrients except for ammonium. On average, dissolved nutrients were 19.65 times higher in concentration at Hythe compared to Mersea. Dissolved nutrient concentrations ( $n = 45$ ) were significantly different across all sites except for ammonium, which did not significantly differ in concentrations across the Colne estuary. Correlational analysis between dissolved nutrients and dissolved hydrocarbon content in the estuary revealed no significant correlations except for dissolved ammonium and methane ( $t_{(7)} = -2.31$ ,  $p = 0.05$ ,  $R^2 = 0.43$ ,  $n = 9$ ).

### 3.3.2 Dissolved methane and ethane concentrations in estuarine water samples

Figure 3.2 shows dissolved methane and ethane concentrations across the study sites in the River Colne. Dissolved methane concentrations were highest at the marine end of the estuary at Mersea ( $85.88 \pm 17.36$  nM CH<sub>4</sub>) whereas the lowest dissolved methane concentration was found mid-estuary at Alresford creek ( $27.75 \pm 14.29$  nM CH<sub>4</sub>). Dissolved ethane concentrations were similar between Hythe ( $631.05 \pm 315.89$  pM C<sub>2</sub>H<sub>6</sub>) and Mersea ( $605.69 \pm 302.84$  pM C<sub>2</sub>H<sub>6</sub>), with a strong mid-estuary dip down to 0 pM ethane at Alresford.

Dissolved methane concentrations differed significantly across study sites

( $F_{(1,2)} = 7.478$ ,  $p = 0.023$ ,  $n = 9$ ). Post-hoc analysis of dissolved methane concentrations across study sites revealed significant differences between Mersea-Alresford and Mersea-Hythe, but not between Hythe-Alresford. No significant interaction between study site and dissolved C<sub>2</sub>H<sub>6</sub> concentration was observed ( $F_{(1,2)} = 1.961$ ,  $p > 0.05$ ).

### 3.3.3 Ex-situ incubations

Figure 3.3 summarises methane headspace concentrations from direct headspace samples from *ex-situ* sediment slurry incubations plotted over the 44 day incubation period. The increase in headspace methane concentrations relative to initial measurements of unamended sediment slurries collected from Hythe increased  $55.67 \pm 72.094$  mM d<sup>-1</sup>,

whereas the inhibited slurries were on average decreasing in headspace methane concentration ( $-75.94 \pm 69.812 \text{ mM CH}_4 \text{ d}^{-1}$ ) while control slurries increased  $0.85 \pm 1.816 \text{ mM d}^{-1}$ . Slurries collected from Alresford creek showed smaller spread in average headspace methane increase per day between treatments compared to Hythe and Mersea slurries. Unamended Alresford slurries increased in headspace methane by  $0.04 \pm 0.158 \text{ mM d}^{-1}$  while inhibited slurries produced  $0.04 \pm 0.092 \text{ mM d}^{-1}$  and control slurries produced  $0.02 \pm 0.116 \text{ mM d}^{-1}$ . Slurries from Mersea, at the mouth of the estuary, showed a larger spread of average headspace methane increase per day between treatments compared to Alresford, but overall much less of a difference than Hythe samples (Unamended:  $0.69 \pm 0.489$ ; Inhibited:  $0.05 \pm 0.074$ ; Control:  $0.06 \pm 0.052 \text{ mM CH}_4 \text{ d}^{-1}$ ).

Slurry methane emissions ( $n = 80$ ) differed significantly between study sites ( $F_{(2,75)} = 5.452, p = 0.0062$ ) and treatments ( $F_{(2,75)} = 6.874, p = 0.001$ ). Post-hoc analysis found significant differences in headspace methane concentrations between Hythe-Alresford and Hythe-Mersea, but not between Mersea-Alresford; while also finding significant differences between Unamended-Control and Unamended-Inhibited samples, but not between Control-Inhibited.

Figure 3.4 summarises ethane headspace concentrations from *ex-situ* sediment slurries incubated for 43 days. Ethane was detected sporadically in trace headspace concentrations in the Hythe unamended and Mersea control treatments in the first 20 days of incubation, then showed a significant increase in the latter 23 days of incubation across all sites and treatments. This observation led to separating the ethane concentration data by incubation time (Fig. 3.4). Overall, the largest ethane concentrations came from Hythe slurries ( $215.97 \pm 12.373 \text{ pM C}_2\text{H}_6$ , averaged from all treatments), followed by Mersea ( $182.86 \pm 66.897 \text{ pM C}_2\text{H}_6$ ) and Alresford ( $141.10 \pm 59.839 \text{ pM C}_2\text{H}_6$ ). No significant differences between site ( $F_{(2,93)} = 1.016, p > 0.05$ ) or treatment ( $F_{(2,93)} = 0.004, p > 0.05$ ) were found for headspace ethane concentrations. However, a significant difference in headspace ethane concentration was observed between the first 20 days of incubation and the last 23

days across all treatments and sites ( $F_{(1,93)} = 26.207$ ,  $p < 0.001$ ), indicating a potentially abiotic process responsible for ethane formation in the sediment slurry incubations.

### 3.3.4 *In-situ hydrocarbon fluxes*

Figure 3.5 summarises methane and ethane fluxes from estuarine sediment and water to the air *in-situ*. Overall, methane fluxes (Fig. 3.5A) were highest at the head of the estuary at Hythe for both the sediment-air ( $56.37 \pm 12.40$  nM CH<sub>4</sub> min<sup>-1</sup> cm<sup>-2</sup>) and water-air interfaces ( $134.73$  nM CH<sub>4</sub> min<sup>-1</sup> cm<sup>-2</sup>,  $n = 1$ ), following a trend of highest fluxes at the head of the estuary then decreasing by the mid-estuary and remaining at this level by the estuary mouth. Methane fluxes differed significantly across study sites ( $F_{(1,2)} = 4.842$ ,  $p = 0.042$ ,  $n = 12$ ) though interface type had no significant interaction with methane flux ( $F_{(1,2)} = 0.013$ ,  $p = 0.913$ ,  $n = 12$ ). Post-hoc analysis revealed only Hythe and Alresford differed significantly in overall flux ( $p = 0.039$ ).

Figure 3.5B shows relatively stable ethane fluxes across Hythe and Alresford at both interfaces, with no ethane fluxes at either interface at Mersea. Sedimentary ethane fluxes at Hythe averaged  $439.91 \pm 19.98$  pM min<sup>-1</sup> cm<sup>-2</sup>, with a very slight decrease at Alresford ( $407.81$  pM min<sup>-1</sup> cm<sup>-2</sup>,  $n = 1$ ). Ethane flux from surface waters at Hythe ( $892$  pM min<sup>-1</sup> cm<sup>-2</sup>,  $n = 1$ ) were almost double that of Alresford ( $483.22 \pm 388.71$  pM min<sup>-1</sup> cm<sup>-2</sup>). Interface type was found to have no significant effect on ethane flux ( $F_{(1,9)} = 0.404$ ,  $p = 0.54$ ,  $n = 12$ ), though fluxes were significantly affected by sample site ( $F_{(2,9)} = 7.931$ ,  $p = 0.01$ ,  $n = 12$ ). Post-hoc analysis showed significant differences only between Mersea-Hythe, though the  $p$ -value was close to the 0.05 threshold when comparing Mersea-Alresford ( $p = 0.08$ ).

### 3.3.5 *Methane – ethane ratios*

Table 3.3 shows calculated C<sub>1</sub>/C<sub>2</sub> ratios from the various measurements in this study. Overall, almost all values exceeded the “Bernard parameter”, exceeding 1000 by several magnitudes, except for dissolved methane and ethane in the water column of the estuary.

The largest  $C_1/C_2$  ratios averaged across all measurements were found at Hythe ( $430311951 \pm 428825616$ ,  $n = 3$ ), followed by Alresford ( $159574615 \pm 59756600$ ,  $n = 3$ ) and Mersea ( $70710550 \pm 57734806$ ,  $n = 3$ ), with the latter two representing ratios 37% and 16% as large as Hythe's ratio. *Ex-situ* sediment slurries produced the largest  $C_1/C_2$  ratio, averaged across all three sites ( $592074555 \pm 474982381$ ,  $n = 3$ ), followed by water-air flux measurements ( $165151179 \pm 92819640$ ,  $n = 2$ ), sediment-air flux ( $117433233 \pm 8747009$ ,  $n = 2$ ) and dissolved in estuarine water ( $128 \pm 10.87$ ,  $n = 2$ ).

The methane – ethane ratio for dissolved hydrocarbons in estuarine water was found to not statistically significantly differ between sites ( $F_{(1,4)} = 0.669$ ,  $p = 0.459$ ,  $n = 8$ ). Ratios produced from flux measurements also did not significantly differ between sites ( $F_{(1,2)} = 0.398$ ,  $p = 0.593$ ,  $n = 8$ ) nor between sediment – air and water – air interfaces ( $F_{(1,2)} = 0.012$ ,  $p = 0.924$ ,  $n = 8$ ).

Table 3.1: Dissolved nutrient concentrations ( $\mu\text{M}$ ) in estuarine water samples from the River Colne estuary, UK. Units are mean values  $\pm$  one standard deviation. ( $n = 3$ )

Site	Nutrient concentration ( $\mu\text{M}$ )				
	$\text{NO}_2^-$	$\text{PO}_4^{3-}$	$\text{NO}_3^-$	Si	$\text{NH}_4^+$
Hythe	$33.87 \pm 0.098$	$35.24 \pm 0.114$	$470.89 \pm 1.918$	$108.22 \pm 0.730$	$2.89 \pm 0.837$
Alresford	$3.40 \pm 0.024$	$5.67 \pm 0.123$	$41.88 \pm 0.054$	$32.09 \pm 0.712$	$4.35 \pm 0.390$
Mersea	$1.01 \pm 0.177$	$4.21 \pm 0.265$	$15.28 \pm 0.726$	$18.39 \pm 3.072$	$3.53 \pm 0.628$

Table 3.2: Physico-chemical parameters from intertidal sediment samples (organic content) and water samples (pH, salinity) collected from the River Colne estuary, UK. Organic content (%) was calculated using ash-free dry weight calculations while pH and salinity were directly measured *in-situ* using a calibrated multiprobe. Values are given  $\pm$  one standard deviation. ( $n = 9$ )

Site	Organic content (%)	pH	Salinity (ppt)
Hythe	$8.08 \pm 1.41$	$9.53 \pm 0.040$	$16.47 \pm 0.586$
Alresford	$5.34 \pm 1.06$	$9.49 \pm 0.050$	$39.70 \pm 0.100$
Mersea	$5.93 \pm 2.80$	$9.59 \pm 0.045$	$40.90 \pm 0.100$

Table 3.3:  $C_1/C_2$  ratios from various measurements in this study. All values were standardised to picomolar (pM) before calculating the ratio. NA indicates no ethane detected for that measurement.

Site	<i>Ex-situ</i> slurry incubations	<i>In-situ</i> sediment-air flux	<i>In-situ</i> water-air flux	Dissolved
Hythe	1541630800	128146087	51470800	115
Alresford	93171908	106720379	278831558	NA
Mersea	141420958	NA	NA	142

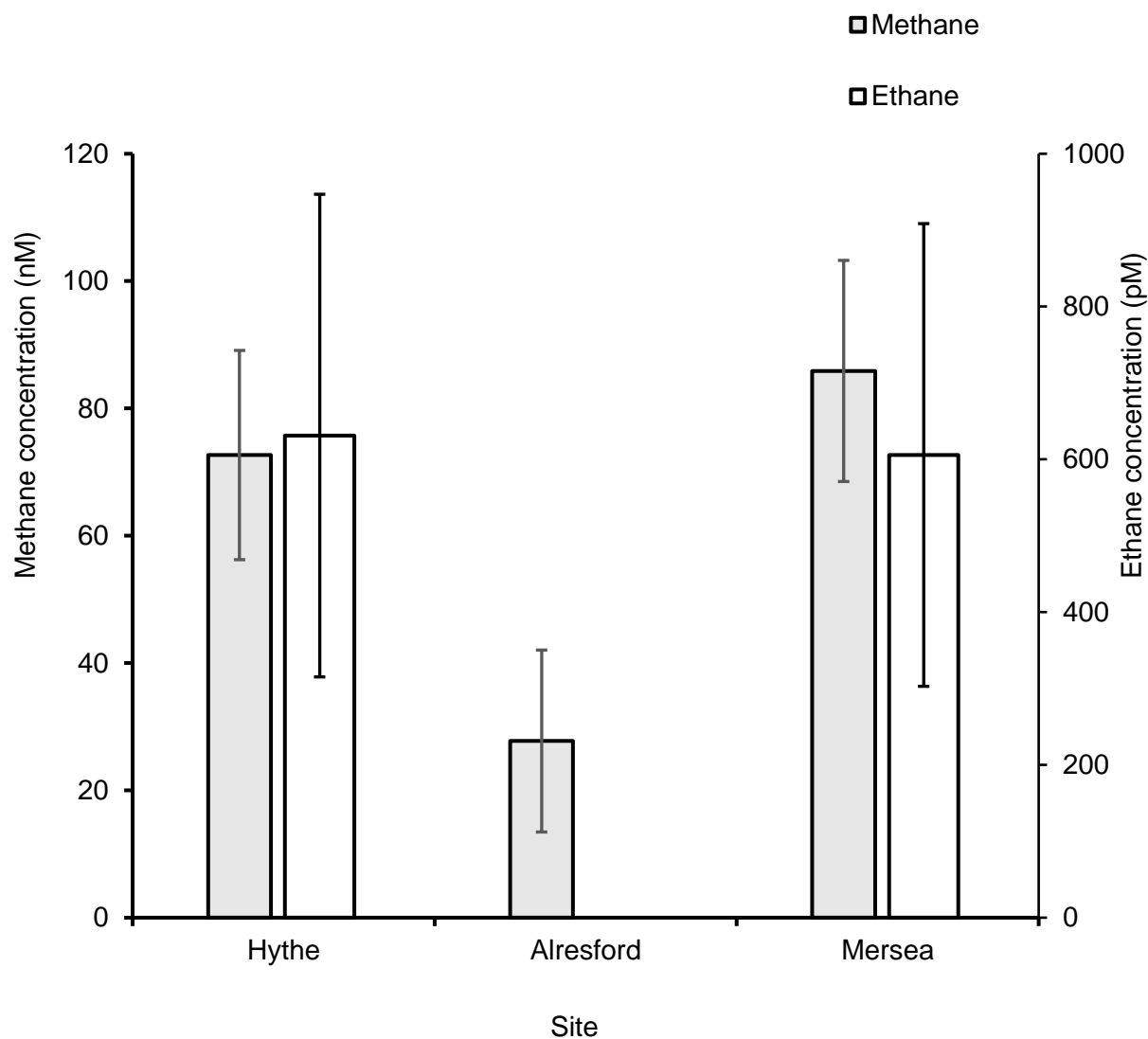


Figure 3.2: Dissolved methane and ethane concentrations in estuarine water samples collected from the River Colne at three sites along its course, ranging from freshwater (salinity < 5 ‰) at the head of the estuary in Hythe, to brackish at Alresford and mostly marine (salinity > 30 ‰) at Mersea. Error bars represent  $\pm$  standard error of the mean (SEM,  $n = 9$ ).

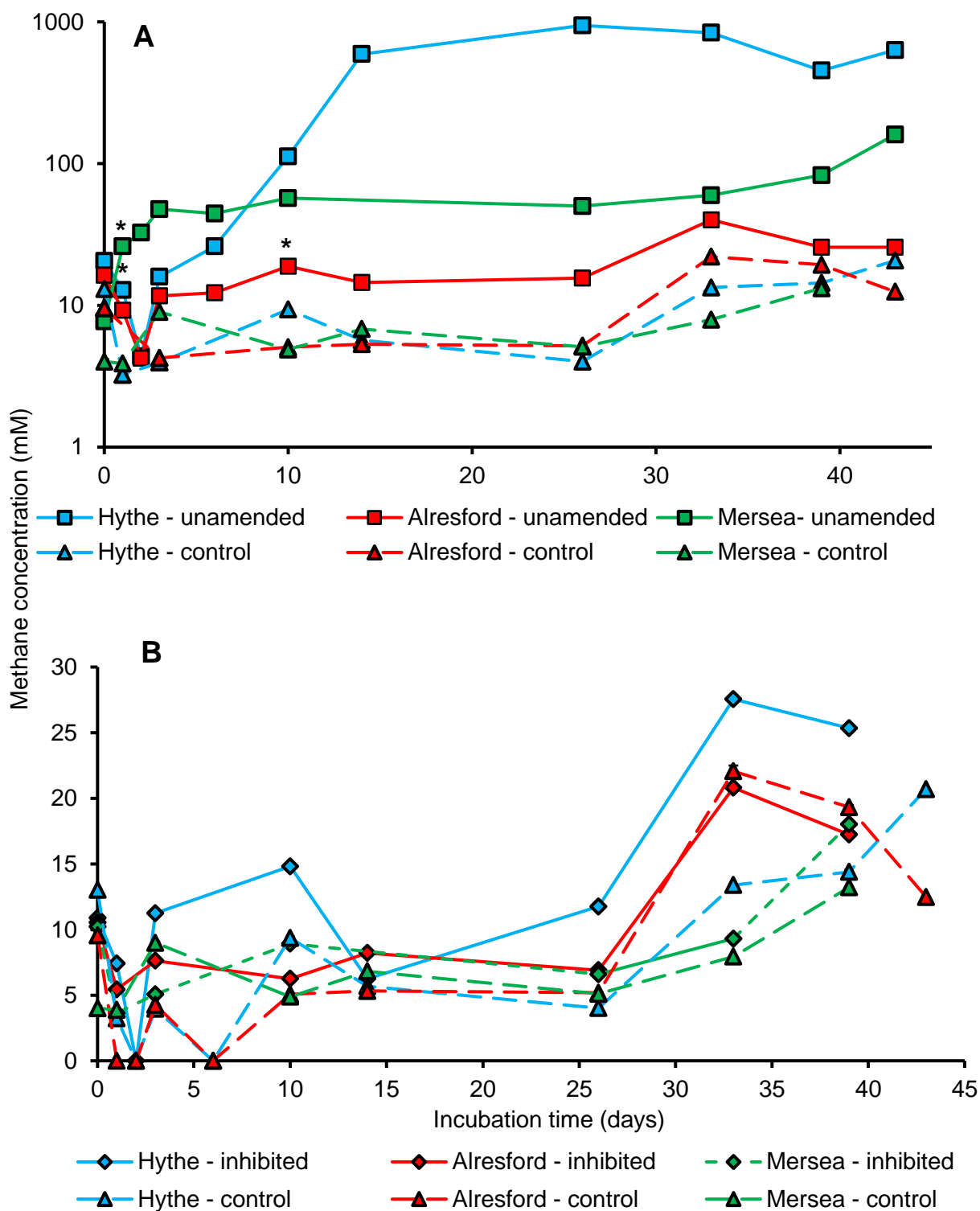


Figure 3.3: Sediment slurry headspace concentrations of methane ( $n = 3$ ) observed over a period of 45 days in the lab. Vials were incubated in the dark with no additions (unamended), 7 mM 2-BES (inhibited) or after autoclaving at 120 °C (abiotic control). **A** – Unamended vials (solid lines) versus abiotic controls (dashed lines). Asterisks indicate when the unamended data became significantly different to the abiotic control data. Methane concentration is presented along a  $\log_{10}$  scale for clarity. **B** – Inhibited vials (solid lines) versus abiotic controls (dashed lines). Data is  $\pm$  SEM, though error bars may be too small to see.

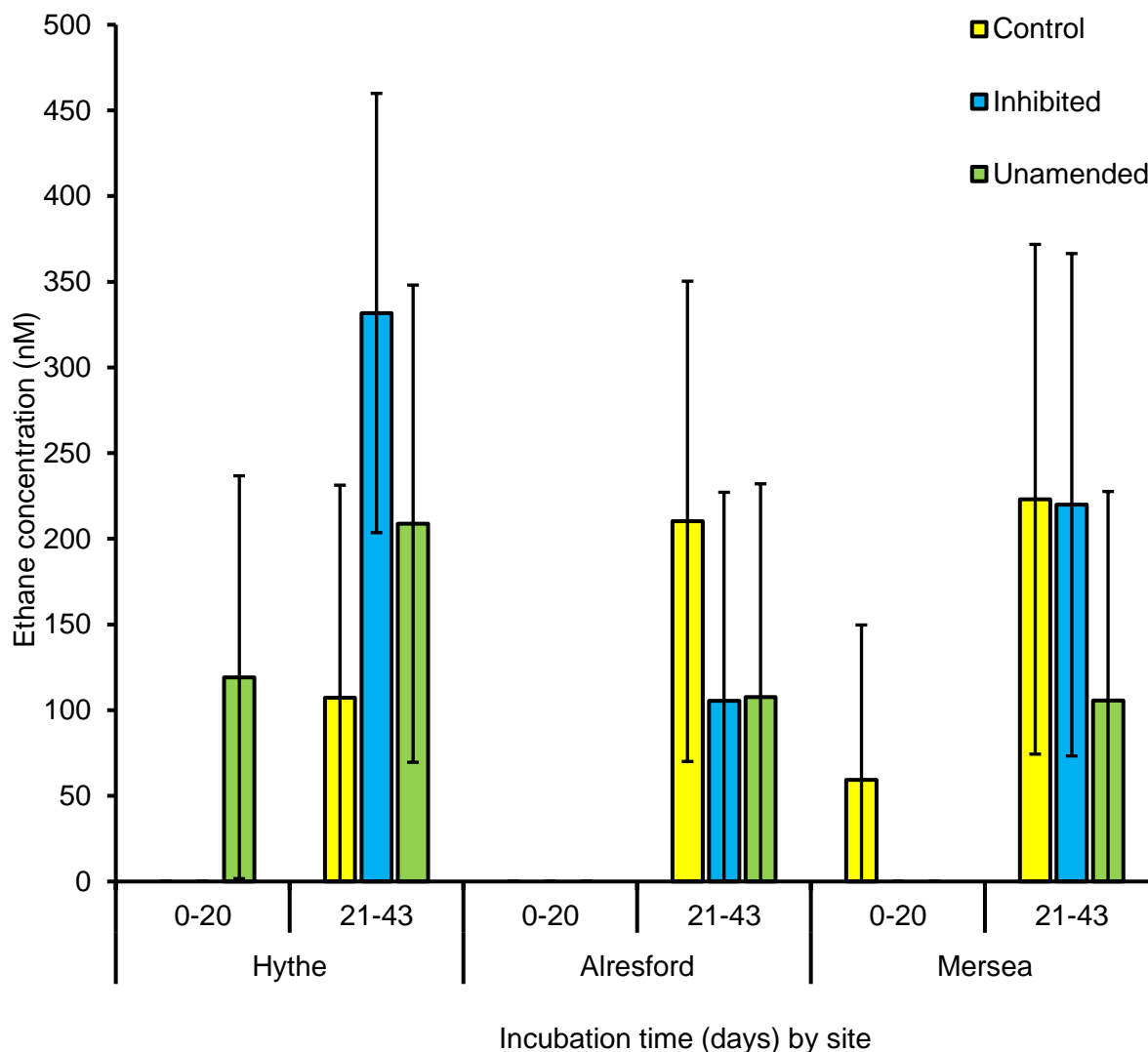


Figure 3.4: Headspace ethane concentrations (nM) from *ex-situ* sediment slurries incubated for 43 days, collected from the River Colne, UK. Three locations were sampled along a salinity gradient (Hythe, at the estuary head; Alresford, a mid-estuary creek and Mersea, at the estuary mouth). Sediment slurries were incubated with no additions (unamended), or with the methanogenesis inhibitor 2-BES at 7 mM (inhibited), or after autoclaving at 120 °C (control). Incubation time is grouped due to statistically significant differences between the initial 20 days and latter 23 days. Data are mean values  $\pm$  SEM.

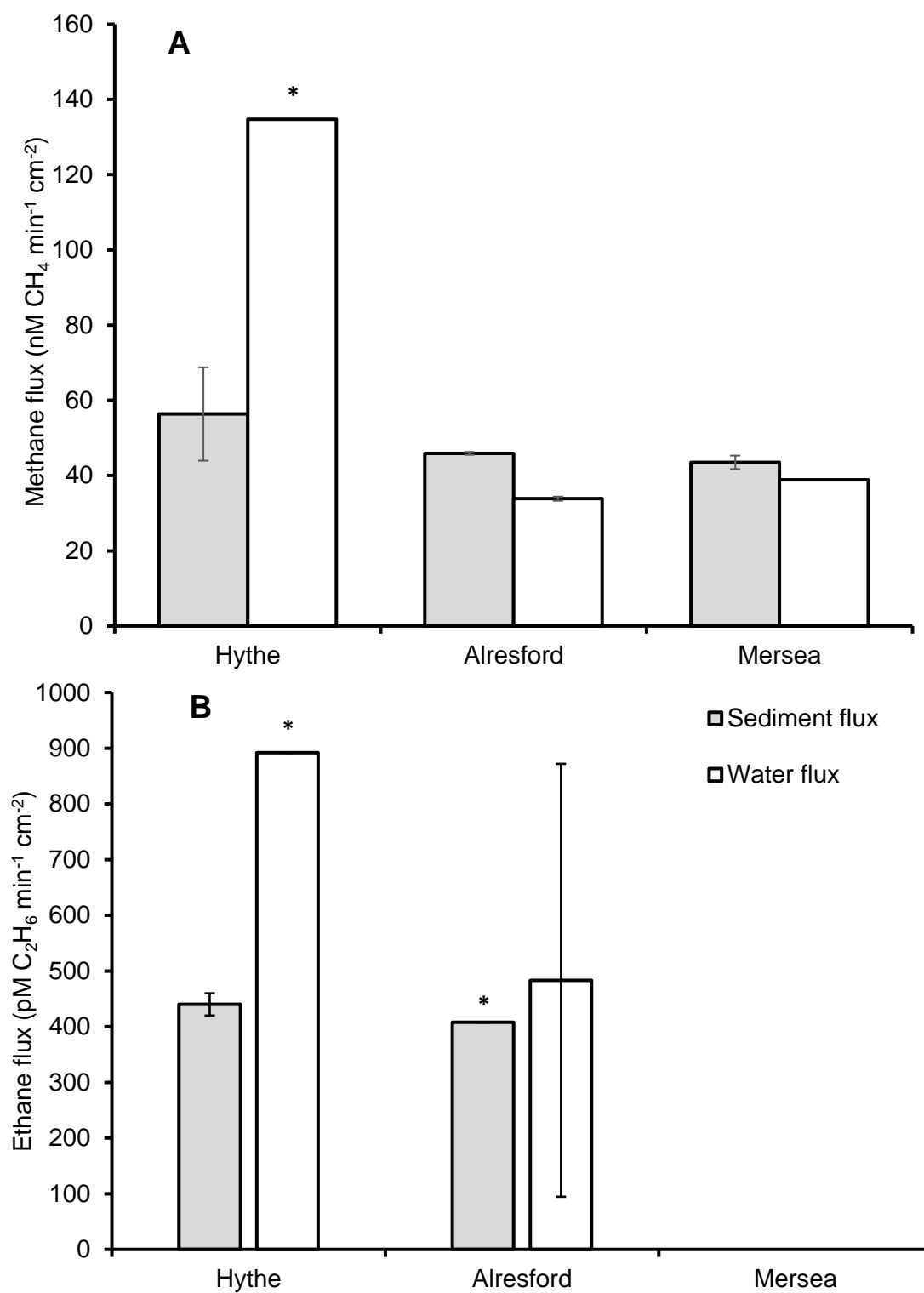


Figure 3.5: Methane (**A**) and ethane (**B**) flux measurements from the River Colne, UK, measured using *in-situ* purpose-built flux chambers (Fig. 2.4) and GC-FID. No ethane flux was found from the Mersea site. Asterisks denote an  $n$  of 1 where appropriate, with an  $n = 3$  for all other values. Values are  $\pm$  standard error.

### 3.4 Discussion

#### 3.4.1 Physico-chemical parameters and their effect on methanogenesis in the Colne estuary

Ammonium ( $\text{NH}_4^+$ ) causes inhibition of methanogenesis in high concentrations, at 1900 – 2000  $\text{mg L}^{-1}$  (Koster, 1986). Ammonia ( $\text{NH}_3$ ) is considered a highly toxic molecule and can be formed when ammonium, which is slightly acidic, reacts with a base to form the unionized ammonia molecule. This reaction is in a chemical equilibrium and can be shifted to produce more ammonia at increased pH. This study found an elevated pH compared to average estuarine pH in the UK (7.0 – 8.6) (EPA, 2009) and to previous measurements in the Colne estuary (Beddow *et al.*, 2014), suggesting an episodic elevation in pH, potentially due to increased primary production or sewage effluent.

This study found a significant negative correlation between ammonium ion concentrations and dissolved methane concentration in the Colne estuary, which has a sewage treatment works outflow near the Hythe sampling site, likely carrying a significant input of ammonium ions in the effluent. Table 3.2 shows the Colne estuary to be fairly alkaline across all study sites, with non-significant ( $p > 0.05$ ) variation between sites, skewing the equilibrium towards creating more ammonia throughout the estuary. Passive diffusion of ammonia into microbial cells causes proton imbalances, potassium deficiency, increased maintenance energy requirements and suppresses specific enzyme reactions (Gallert *et al.*, 1998), which may be inhibiting methanogenesis in the Colne estuary. However, counter evidence suggests methanogens can survive ammonium in concentrations exceeding 1000  $\text{mg L}^{-1}$  (Esquivel-Elizondo *et al.*, 2016), suggesting ammonium concentrations in the estuary may be a poor predictor for overall methanogenic activity.

Organic content in sediments has been hypothesised to influence methanogenic community compositions and overall methane production through the methanogenesis-substrate supply model, which suggests substrates derived from settling autochthonous organic matter explains variations in methane production (West *et al.*, 2016). However, there were no significant differences in sedimentary organic content between sites in the Colne estuary

(Table 3.2), suggesting this to be a poor predictor for methane production. Bertolet *et al.* (2019) find organic matter in lake sediments to explain variations in methanogenic community compositions, though it does not explain variations in methanogenesis rates. Rather, variations in methanogenesis rates were best explained by proxies for organic content such as lake chlorophyll-*a* content, further suggesting overall carbon content in sediments is a poor predictor of methanogenic production.

#### 3.4.2 Contextualising dissolved hydrocarbon dynamics in the Colne estuary

Dissolved methane concentrations were highest in Mersea, followed by Hythe and a marked mid-estuary minimum at Alresford (Fig. 3.2). Previous research identified *Methanosarcinales* as the predominant methanogenic order in surface (< 2 cm) sediments at Alresford which contained a diverse community of methylotrophic (*Methanosarcina*, *Methanococcoides*), acetotrophic (*Methanosarcina*, *Methanosaeta*) and hydrogenotrophic (*Methanomicrobiales*) methanogens (Webster *et al.*, 2015). Methanogen populations in Hythe are dominated by obligate hydrogenotrophic and acetoclastic microbes (*Methanosaeta*), whereas marine surface sediments in Brightlingsea (located close to Mersea Island) had a high proportion of *Methanococcoides*, *Methanolobus* and *Methanosarcina* species, which are all able to utilize non-competitive methyl substrates (Webster *et al.*, 2015). These changes in community structure reflect the dynamic estuarine environment where salinity affects which methanogens are most competitively viable at each site.

Broadgate *et al.* (2004) examined dissolved non-methane hydrocarbon concentrations in tidal rockpools on the western coast of Ireland, finding 26.3 – 44.2 pM C<sub>2</sub>H<sub>6</sub> in rockpools and 32.0 pM C<sub>2</sub>H<sub>6</sub> in seawater collected 3 km from the coast. Riemer *et al.* (2000) found 179 pM C<sub>2</sub>H<sub>6</sub> dissolved in coastal seawater from Shark River, Florida. This study found on average ~600 pM C<sub>2</sub>H<sub>6</sub> in the Colne estuary samples, markedly higher than most other studies, most likely due to elevated levels of primary production due to hypereutrophication from the sewage treatment works effluent. Lomond and Tong (2011) found 864 pM C<sub>2</sub>H<sub>6</sub> dissolved in a pond sampled in Nova Scotia, though acknowledge ethane as below

quantification limits in multiple samples, nonetheless finding similar concentrations to those found in this study.

Short chain non-methane hydrocarbons (NMHC) may share a relationship with phytoplankton growth cycles. Qualitative evidence shows NMHC are in highest concentrations in the euphotic zone in oxygenated marine waters (Macdonald, 1976). Lee and Baker (1992) examined ethylene and ethane production in an estuary, finding increased ethane production in sunlit conditions compared to dark. Ethane is among the products created from photo-decomposition of polyunsaturated fatty acids, which was shown by adding linolenic acid to estuarine water samples and observing an increase in ethane (and ethylene) production compared to acid-free samples (Lee and Baker, 1992). Sterilized samples prior to sunlit incubation for 8 hours reached 0.09 nM, which may be due to decomposition of cellular polyunsaturated fatty acids, which are no longer protected against photolysis by protective enzyme systems found in living cells (Lee and Baker, 1992). McKay *et al.* (1996) observed NMHC production in axenic cultures of representative species from diatoms (Bacillariophyceae) and dinoflagellates (Dinophyceae), with the majority of production following chlorophyll-*a* peaks indicating that production in the cultures was related in some way to the organics produced by the degradation of plankton cells. Ethane was observed in three-fold higher concentrations in bottles with *Skeletonema costatum* than in blank (abiotic) bottles, although the evidence was inconclusive for ethane production in dinoflagellate cultures. These findings suggest short chain NMHC are produced during the degradation of planktonic matter.

Chlorophyll-*a* concentrations in the Colne estuary vary by site, between 0.5  $\mu\text{g L}^{-1}$  (Brightlingsea) and 37.5  $\mu\text{g L}^{-1}$  (Hythe), as well as seasonally, peaking in July (Kocum *et al.*, 2002), which would imply dissolved ethane concentrations should be highest at Hythe and lowest in Brightlingsea if all of the ethane was formed from photolysis of free polyunsaturated acids originating in planktonic cells. However, this study found the lowest dissolved ethane concentration (zero) at Alresford (Fig. 3.2), with no significant differences

between sites. Webster *et al.* (2015) analysed the diversity of archaeal 16S rRNA gene sequences from Colne estuary sediments, finding a larger proportion of Bathyarchaeota compared to other Archaea in Alresford sediments compared to Hythe and Brightlingsea sediments, while also finding the highest concentrations of volatile fatty acids in Alresford, though overall concentrations of volatile fatty acids were low across the entire estuary ( $< 43 \mu\text{M}$ ). Non-Euryarchaeotal methanogenesis is often identified by targeting the *mcrA* gene, which can be misleading as the methyl-coenzyme M reductase complex catalyses the first step in methanotrophy as well as the final step in methanogenesis, while divergent *mcr*-like genes have been shown to catalyse short-chain alkane breakdown (Evans *et al.*, 2019), suggesting the Bathyarchaeota Archaea found in Alresford sediments may be non-methanogenic. Non-Euryarchaeotal methanogenesis is mostly methylotrophic (Berghuis *et al.*, 2019), while all observed ethanogenesis comes from hydrogenotrophic methanogens, suggesting the lower dissolved ethane concentrations may be due to a lack of ethanogenic Archaea in Alresford sediments as well as low available fatty acids for photolytic production of ethane.

### 3.4.3 Hydrocarbon fluxes in the Colne Estuary

Estuaries are a significant source of methane to the atmosphere globally, with very little research on ethane emissions. De Angelis and Lilley (1987) find an average of  $0.18 \text{ mM m}^{-2} \text{ d}^{-1} \text{ CH}_4$  flux from surface waters of Oregon rivers and estuaries measured over a 4 year period, while Middelburg *et al.* (2002) find an average of  $0.13 \text{ mM m}^{-2} \text{ d}^{-1} \text{ CH}_4$  flux from 9 European estuaries. Extrapolating the data from this study, estimates of 1940.26, 487.58 and 559.58  $\text{mM m}^{-2} \text{ d}^{-1} \text{ CH}_4$  for water-air flux and 811.73, 661.10 and 626.69  $\text{mM m}^{-2} \text{ d}^{-1} \text{ CH}_4$  sedimentary flux from Hythe, Alresford and Mersea respectively can be obtained. These values range from  $7.82 - 31.12 \text{ g CH}_4 \text{ m}^{-2} \text{ d}^{-1}$  released to the atmosphere, which is very high relative to other studies. Chen *et al.* (2017) studied ebullitive flux of methane from an estuarine mudflat over multiple tidal cycles using a deployed *in-situ* flow-through chamber connected to a real time methane analyser, finding an average of

1.3 g CH<sub>4</sub> m<sup>-2</sup> d<sup>-1</sup> released to the atmosphere. The lower value found by Chen *et al.* (2017) shows that extrapolating data from short-term flux chamber deployment at low tide may overestimate daily emissions as methane will be attenuated by microbial and geochemical activity in the water column during tidal movement, as well as masking significant effects from wind activity. This suggests methane flux from the Colne estuary may be ebullitive rather than diffusive, due to the unusually large flux values. Tidal movements will affect ebullitive flux of trapped sedimentary gases induced by changes in pore water pressure as a result of tidal variations and the resulting gas release from the surface both across daily and seasonal time scales, meaning tidal activity has a correlation with overall methane release from the estuarine environment (Chen *et al.*, 2017). Increased global temperatures due to climate change will substantially increase methane flux from natural wetland environments by as much as 20% with a 1 °C increase (Shindell *et al.*, 2004), further illustrating a need to understand methane release dynamics across tidal environments.

Li *et al.* (2019) found an average sea-to-air flux of  $6.6 \pm 7.1$  nmol C<sub>2</sub>H<sub>6</sub> m<sup>-2</sup> d<sup>-1</sup> in the western Pacific Ocean, which is two orders of magnitude higher than the fluxes measured in this study, suggesting overall ethane emissions from the Colne estuary are lower than fully marine flux. The low values for ethane flux compared with the very high values for methane flux coupled with the large methane – ethane ratios strongly suggests biogenic production of methane in the estuary.

#### 3.4.4 Sedimentary hydrocarbon production

Oremland *et al.* (1981) found  $634 \pm 398$  mM CH<sub>4</sub> and  $2.4 \pm 1.4$  μM C<sub>2</sub>H<sub>6</sub> after incubating sediment for 39 days in flasks with a H<sub>2</sub>-rich headspace. Oremland *et al.* (1981) findings place the methane production from San Francisco bay sediments in a similar range to the Hythe sediments, which reached  $632.90 \pm 40.73$  mM CH<sub>4</sub> after 43 days of incubation, suggesting methanogenic production in both estuarine sediments may be enhanced due to eutrophication, as Hythe is located at a sewage treatment works outflow. The large methane – ethane ratios for sediment slurries (Table 3.3), coupled with inhibition of methane

formation in vials incubated with the methanogenesis inhibitor 2-BES shows strong evidence for microbial formation of methane in Colne sediments.

This study found 50 – 350 nM C<sub>2</sub>H<sub>6</sub> after 43 days of incubation with a H<sub>2</sub> and CO<sub>2</sub> rich headspace, which is several orders of magnitude lower than Oremland *et al* (1981) findings, though this may be due to an abundance of available H<sub>2</sub> in glass syringes in Oremland *et al* (1981). In another study, Oremland *et al.* (1988) found 13 – 125 nM headspace ethane from sediment slurry incubations from various aquatic environments, placing these results in the same range as this study. Oremland *et al.* (1988) found that H<sub>2</sub> had a paradoxical effect on ethane formation, whereby in some samples incubated with H<sub>2</sub> the ethane formation was enhanced, whereas in others it was inhibited. The authors suggest this may be due to differences in methanogenic flora between sites, where additions of H<sub>2</sub> would have enriched for H<sub>2</sub>-oxidizing methanogens (which do not use methylated compounds) at the expense of the obligate methylotrophs, which would affect the overall ethane formation.

This study found ethane formation across all treatments, including inhibited and control samples, contradicting the evidence found in Oremland *et al.* (1981) and Oremland *et al.* (1988). Ethane formation was markedly higher after the first 20 days of incubation across all treatments and sites, suggesting a delayed abiotic process is responsible for ethane formation in Colne estuary sediments. Photolytic decomposition of volatile fatty acids seems likely, though samples were incubated in the dark with only brief periods of being exposed to light. This may have led to the delayed formation of ethane, though it would be expected to see more immediate formation of ethane in autoclaved samples, where volatile fatty acids from “burst” benthic plankton and microbial life would be unprotected from photolysis.

## Chapter 4 – Summary

### 4.1 – Conclusions based on findings from the study

This study quantified methane and ethane fluxes from sediment – air and water – air interfaces across the Colne estuary, as well as dissolved in estuarine water and produced from sediment slurries *ex-situ*. An inventory of methane – ethane ratios from the Colne estuary has been produced (Table 3.3), which can be used to inform future studies, particularly with relevance to contemporary astrobiological research.

Revisiting the hypotheses laid out in chapter 3.1.2, it has been observed:

- a) Dissolved methane was highest at Hythe and Mersea, with a mid-estuary dip in concentration. Concentrations were found to significantly differ between the head of the estuary (Hythe) and the mouth (Mersea), but not between the mid-estuary (Alresford) and the head, though the mouth and the mid – estuary differed. Dissolved ethane was found in similar concentrations at Hythe and Mersea, with no dissolved ethane found in Alresford. No significant statistical interaction between sample site and ethane concentrations were found.
- b) Headspace methane concentrations in *ex-situ* sediment slurry incubations were significantly lower in vials incubated with the methanogenesis inhibitor 2-BES and in vials that were autoclaved compared with unamended slurries. Significant statistical differences were observed between unamended vials and inhibited/control vials, but not between inhibited and control vials.

- c) Headspace methane concentrations were highest in Hythe sediment slurries, followed by Mersea with a mid-estuary minimum at Alresford. Significant statistical differences were observed between Hythe and Alresford/Mersea, but not between Alresford and Mersea.
- d) Headspace ethane concentrations from sediment slurry incubations were overall similar across all sites and treatments, with no significant differences observed in either. However, ethane concentrations were observed to increase over the incubation period, with a statistical difference in ethane concentrations between the first 20 days of incubation and the latter 20 days.
- e) Methane and ethane fluxes from the Colne estuary were quantified across sediment – air and water – air interfaces, finding the highest methane fluxes from both interfaces at Hythe, with similar methane fluxes from Alresford and Mersea across both interfaces. Ethane fluxes were highest at Hythe, followed by Alresford with no fluxes found at Mersea.
- f) Methane – ethane ratios were calculated for all measurement types, finding very high values (>1000) across all measurements except for dissolved methane – ethane ratios, which ranged from 115 – 142.

#### *4.2 – Improvement suggestions for future studies*

Quantifying methane and ethane in the dynamic estuarine environment presented many unique challenges. Ethane is a trace gas, usually found in the picomolar range in the environment, meaning rigorous methods must be used to ensure no contamination occurs. Dissolved methane and ethane in water samples were difficult to quantify, due to ethane's trace nature and methane not cryogenically enriching. Future studies could employ purge-and-trap apparatus with cryogenic loops with glass beads, such as in Broadgate *et al.* (1997), or purpose-built apparatus with higher desorb temperature and heated transfer lines (e.g. Chambers *et al.*, 2012) during analysis to potentially cryogenically enrich methane.

An unsuccessful aqueous calibration for methane in water samples was performed in this study by bubbling 99% CH<sub>4</sub> standard (BOC, UK) into a 2 L glass conical flask filled with 1 L sterile artificial sea water for 1 hour (after Chambers *et al*, 2012), kept cool in a cool box filled with ice to ensure maximum solubility of methane. The stock solution of artificial sea water saturated with methane was assumed to be 39.6 ppm (the maximum solubility of methane in sea water), which was then diluted to 0 – 2 ppm standards in gas-tightly sealed 20 mL glass vials. However, the standards were found to not correlate with calculated concentrations via this method, most likely due to the high pressure from the standard gas bottle allowing for higher saturation of methane in the artificial sea water. Future studies could attempt to create an aqueous calibration standard for methane in artificial sea water by allowing methane to equalise to standard atmospheric pressure via a gas bladder (e.g. p/n 11734498, Fisher, UK), then introducing the methane standard into a gas-tightly sealed vial with a 1:1 ratio of artificial sea water and headspace. The methane will then equilibrate over time, resulting in a stock solution saturated with methane, which can then be diluted as necessary to create a linear calibration series. A zero-hydrocarbon water sample for control purposes could potentially be created by pulling a vacuum on an artificial sea water sample connected in-line with a hydrocarbon trap.

#### 4.3 Summary

This study set out to develop an inventory of methane – ethane ratios from a dynamic estuarine environment for informative purposes in future studies which need to discriminate between biogenic and non-biogenic methane via investigating atmospheric compositions of gases, particularly in the context of astrobiological studies. A range of ratios have been produced from multiple measurement types (Table 3.3), along with methods developed for quantification of methane and ethane from environmental samples. These ratios can be utilised by astrobiologists, alongside ratios from geologically produced methane on Earth, to constrain extra-terrestrial methane using instruments such as the ExoMars orbiter. This

study quantified aqueous methane measurements, which may shed light on methane origins in water plumes on Enceladus and Europa.

Future studies can use further constraints (e.g.  $\delta^{13}\text{C}/\delta^{12}\text{C}$ ; deuterium/hydrogen measurements) to create a multidimensional data set for informative purposes.

## References

Adams, D. F., Farwell, S. O., Robinson, E. and Pack, M. R. (1980) *Biogenic sulfur emissions in the SURE regions ( USA)*. U.S. Department of Energy.

Ainsworth, E. A., Yendrek, C. R., Sitch, S., Collins, W. J. and Emberson, L. D. (2012) 'The Effects of Tropospheric Ozone on Net Primary Productivity and Implications for Climate Change', *Annual Review of Plant Biology*, **63**, 637–661.

Anenberg, S. C., Horowitz, L. W., Tong, D. Q. and West, J. J. (2010) 'An estimate of the global burden of anthropogenic ozone and fine particulate matter on premature human mortality using atmospheric modeling', *Environmental Health Perspectives*, **118**, 1189–1195.

de Angelis, M. A. and Lilley, M. D. (1987) 'Methane in surface waters of Oregon estuaries and rivers<sup>1</sup>', *Limnology and Oceanography*. John Wiley & Sons, Ltd, **32**, 716–722.

Bartlett, K. B., Bartlett, D. S., Harriss, R. C. and Sebacher, D. I. (1987) 'Methane emissions along a salt marsh salinity gradient', *Biogeochemistry*. Martinus Nijhoff/Dr. W. Junk Publishers, **4**, 183–202.

Beddow, J., Stölpe, B., Cole, P. A., Lead, J. R., Sapp, M., Lyons, B. P., McKew, B., Steinke, M., Benyahia, F., Colbeck, I. and Whitby, C. (2014) 'Estuarine sediment hydrocarbon-degrading microbial communities demonstrate resilience to nanosilver', *International Biodeterioration and Biodegradation*. Elsevier Ltd, **96**, 206–215.

Berghuis, B. A., Yu, F. B., Schulz, F., Blainey, P. C., Woyke, T. and Quake, S. R. (2019) 'Hydrogenotrophic methanogenesis in archaeal phylum Verstraetearchaeota reveals the shared ancestry of all methanogens', *Proceedings of the National Academy of Sciences of the United States of America*. National Academy of Sciences, **116**, 5037–5044.

Bernard, B. (1978) 'Light Hydrocarbons in Marine Sediments', *Deep-Sea Research*, **26**, 429–443.

Bernhard, A. E. and Bollmann, A. (2010) 'Estuarine nitrifiers: New players, patterns and

processes', *Estuarine, Coastal and Shelf Science*. Academic Press, **88**, 1–11.

Bertolet, B. L., West, W. E., Armitage, D. W. and Jones, S. E. (2019) 'Organic matter supply and bacterial community composition predict methanogenesis rates in temperate lake sediments', *Limnology and Oceanography Letters*. Wiley, **4**, 164–172.

Borges, A. V., Darchambeau, F., Teodoru, C. R., Marwick, T. R., Tamooch, F., Geeraert, N., Omengo, F. O., Guérin, F., Lambert, T., Morana, C., Okuku, E. and Bouillon, S. (2015) 'Globally significant greenhouse-gas emissions from African inland waters', *Nature Geoscience*. Nature Publishing Group, **8**, 637–642.

Bose, A., Rogers, D. R., Adams, M. M., Joye, S. B. and Girguis, P. R. (2013) 'Geomicrobiological linkages between short-chain alkane consumption and sulfate reduction rates in seep sediments', *Frontiers in Microbiology*. Frontiers Research Foundation, **4**, 386.

Bouquet, A., Mousis, O., Waite, J. H. and Picaud, S. (2015) 'Possible evidence for a methane source in Enceladus' ocean', *Geophysical Research Letters*. John Wiley & Sons, Ltd, **42**, 1334–1339.

Broadgate, W. J., Liss, P. S. and Penkett, S. A. (1997) 'Seasonal emissions of isoprene and other reactive hydrocarbon gases from the ocean', *Geophysical Research Letters*. American Geophysical Union, **24**, 2675–2678.

Broadgate, W. J., Malin, G., Küpper, F. C., Thompson, A. and Liss, P. S. (2004) 'Isoprene and other non-methane hydrocarbons from seaweeds: A source of reactive hydrocarbons to the atmosphere', *Marine Chemistry*, **88**, 61–73.

Camacho, A., Picazo, A., Rochera, C., Santamans, A. C., Morant, D., Miralles-Lorenzo, J. and Castillo-Escrivà, A. (2017) 'Methane emissions in Spanish saline lakes: Current rates, temperature and salinity responses, and evolution under different climate change scenarios', *Water (Switzerland)*, **9**, 1–20.

CHAMBERS, L., ENGELHART, G. and HAZARD, S. (2012) 'Purge-and-Trap GC Analysis of

Methane in Water Samples Associated with Hydraulic Fracturing', *LC GC North America*.

Chen, X., Schäfer, K. V. R. and Slater, L. (2017) 'Methane emission through ebullition from an estuarine mudflat: 2. Field observations and modeling of occurrence probability', *Water Resources Research*. Blackwell Publishing Ltd, **53**, 6439–6453.

Claypool, G. . (1999) 'AAPG Hedberg Conference Abstracts', *Natural Gas Formation and Occurrence*, 27–29.

Conrad, R. (2007) 'Microbial Ecology of Methanogens and Methanotrophs', *Advances in Agronomy*. Academic Press, 1–63.

Conrad, R. (2009) 'The global methane cycle: Recent advances in understanding the microbial processes involved', *Environmental Microbiology Reports*. Environ Microbiol Rep, 285–292.

Conrad, R. and Rothfuss, F. (1991) 'Methane oxidation in the soil surface layer of a flooded rice field and the effect of ammonium', *Biology and Fertility of Soils*. Springer-Verlag, **12**, 28–32.

Conrad, R. and Seiler, W. (1980) 'Contribution of hydrogen production by biological nitrogen fixation to the global hydrogen budget.', *Journal of Geophysical Research*. John Wiley & Sons, Ltd, **85**, 5493–5498.

Cui, M., Ma, A., Qi, H., Zhuang, X. and Zhuang, G. (2015) 'Anaerobic oxidation of methane: An "active" microbial process', *MicrobiologyOpen*. Blackwell Publishing Ltd, 1–11.

Daffonchio, D. *et al.* (2006) 'Stratified prokaryote network in the oxic–anoxic transition of a deep-sea halocline', *Nature*, **440**, 203–207.

Dlugokencky, E. J. (2018) *Global methane trends*, NOAA. Available at: [www.esrl.noaa.gov/gmd/ccgg/trends\\_ch4/%0A%0A](http://www.esrl.noaa.gov/gmd/ccgg/trends_ch4/%0A%0A) (Accessed: 17 January 2019).

Donval, J. P. and Guyader, V. (2017) 'Analysis of hydrogen and methane in seawater by

“Headspace” method: Determination at trace level with an automatic headspace sampler’, *Talanta*. Elsevier B.V., **162**, 408–414.

Dougherty, M. K., Khurana, K. K., Neubauer, F. M., Russell, C. T., Saur, J., Leisner, J. S. and Burton, M. E. (2006) ‘Identification of a Dynamic Atmosphere at Enceladus with the Cassini Magnetometer’, *Science*. American Association for the Advancement of Science, **311**, 1406–1409.

Eklund, B. (1992) ‘Practical guidance for flux chamber measurements of fugitive volatile organic emission rates’, *Journal of the Air and Waste Management Association*, **42**, 1583–1591.

Encinas Fernández, J., Peeters, F. and Hofmann, H. (2014) ‘Importance of the autumn overturn and anoxic conditions in the hypolimnion for the annual methane emissions from a temperate lake’, *Environmental Science and Technology*, **48**, 7297–7304.

Esquivel-Elizondo, S., Parameswaran, P., Delgado, A. G., Maldonado, J., Rittmann, B. E. and Krajmalnik-Brown, R. (2016) ‘Archaea and Bacteria Acclimate to High Total Ammonia in a Methanogenic Reactor Treating Swine Waste’, *Archaea*. Hindawi Limited, **2016**, 10.

Evans, P. N., Boyd, J. A., Leu, A. O., Woodcroft, B. J., Parks, D. H., Hugenholtz, P. and Tyson, G. W. (2019) ‘An evolving view of methane metabolism in the Archaea’, *Nature Reviews Microbiology*. Nature Publishing Group, 219–232.

Evans, P. N., Parks, D. H., Chadwick, G. L., Robbins, S. J., Orphan, V. J., Golding, S. D. and Tyson, G. W. (2015) ‘Methane metabolism in the archaeal phylum Bathyarchaeota revealed by genome-centric metagenomics’, *Science*, **350**, 434–438.

Franchini, F. and Steinke, M. (2016) ‘Protocols for the Quantification of Dimethyl Sulfide (DMS) and Other Volatile Organic Compounds in Aquatic Environments’, in *Hydrocarbon and Lipid Microbiology protocols*. Springer, Berlin, Heidelberg, 161–177.

Gallert, C., Bauer, S. and Winter, J. (1998) ‘Effect of ammonia on the anaerobic degradation

- of protein by a mesophilic and thermophilic biowaste population', *Applied Microbiology and Biotechnology*. Springer, **50**, 495–501.
- Grossart, H.-P., Frindte, K., Dziallas, C., Eckert, W. and Tang, K. W. (2011) 'Microbial methane production in oxygenated water column of an oligotrophic lake', *Proceedings of the National Academy of Sciences*, **108**, 19657–19661.
- Gvakharia, A., Kort, E. A., Brandt, A., Peischl, J., Ryerson, T. B., Schwarz, J. P., Smith, M. L. and Sweeney, C. (2017) 'Methane, Black Carbon, and Ethane Emissions from Natural Gas Flares in the Bakken Shale, North Dakota', *Environmental Science and Technology*, **51**, 5317–5325.
- Hammerschmidt, S. B., Wiersberg, T., Heuer, V. B., Wendt, J., Erzinger, J. and Kopf, A. (2014) 'Real-time drilling mud gas monitoring for qualitative evaluation of hydrocarbon gas composition during deep sea drilling in the Nankai Trough Kumano basin', *Geochemical Transactions*, **15**, 15.
- Hanson, R. and Hanson, T. (1996) 'Methanotrophic Bacteria', *Microbiological reviews*, **60**, 439–471.
- Hinrichs, K.-U., Hayes, J. M., Bach, W., Spivack, A. J., Hmelo, L. R., Holm, N. G., Johnson, C. G. and Sylva, S. P. (2006) 'Biological formation of ethane and propane in the deep marine subsurface', *Proceedings of the National Academy of Sciences*. National Academy of Sciences, **103**, 14684–14689.
- Hodges, C. F. and Campbell, D. A. (1998) 'Gaseous hydrocarbons associated with black layer induced by interaction of cyanobacteria and *Desulfovibrio desulfuricans*', *Plant and Soil*. Kluwer Academic Publishers, **205**, 77–83.
- Karl, D. M., Beversdorf, L., Björkman, K. M., Church, M. J., Martinez, A. and Delong, E. F. (2008) 'Aerobic production of methane in the sea', *Nature Geoscience*. Nature Publishing Group, **1**, 473–478.

- Kinnaman, F. S., Valentine, D. L. and Tyler, S. C. (2007) 'Carbon and hydrogen isotope fractionation associated with the aerobic microbial oxidation of methane, ethane, propane and butane', *Geochimica et Cosmochimica Acta*, **71**, 271–283.
- Kirschke, S. *et al.* (2013) 'Three decades of global methane sources and sinks', *Nature Geoscience*, 813–823.
- Kniemeyer, O., Musat, F., Sievert, S. M., Knittel, K., Wilkes, H., Blumenberg, M., Michaelis, W., Classen, A., Bolm, C., Joye, S. B. and Widdel, F. (2007) 'Anaerobic oxidation of short-chain hydrocarbons by marine sulphate-reducing bacteria', *Nature*. Nature Publishing Group, **449**, 898–901.
- Knies, J., Damm, E., Gutt, J., Mann, U. and Pinturier, L. (2004) 'Near-surface hydrocarbon anomalies in shelf sediments off Spitsbergen: Evidences for past seepages', *Geochemistry, Geophysics, Geosystems*. John Wiley & Sons, Ltd, **5**.
- Kocum, E., Underwood, G. J. C. and Nedwell, D. B. (2002) 'Simultaneous measurement of phytoplanktonic primary production, nutrient and light availability along a turbid, eutrophic UK east coast estuary (the Colne Estuary)', *Marine Ecology Progress Series*. Inter-Research, **231**, 1–12.
- Koene-Cottaar, F. H. . and Schraa, G. (1998) 'Anaerobic reduction of ethene to ethane in an enrichment culture', *FEMS Microbiology Ecology*. Oxford University Press, **25**, 251–256.
- Korablev, O. *et al.* (2019) 'No detection of methane on Mars from early ExoMars Trace Gas Orbiter observations', *Nature*. Nature Publishing Group, **568**, 517–520.
- Koster, I. W. (1986) 'Characteristics of the pH-influenced adaptation of methanogenic sludge to ammonium toxicity', *Journal of Chemical Technology & Biotechnology*, **36**, 445–455.
- Krasnopolsky, V. A. (2012) 'Search for methane and upper limits to ethane and SO<sub>2</sub> on Mars', *Icarus*. Elsevier Inc., **217**, 144–152.
- Kristjansson, J. K. and Schönheit, P. (1983) 'Why do sulfate-reducing bacteria outcompete

- methanogenic bacteria for substrates?', *Oecologia*. Springer-Verlag, **60**, 264–266.
- Lee, R. F. and Baker, J. (1992) 'Ethylene and ethane production in an estuarine river: formation from the decomposition of polyunsaturated fatty acids', *Marine Chemistry*. Elsevier, **38**, 25–36.
- Li, J. L., Zhai, X., Ma, Z., Zhang, H. H. and Yang, G. P. (2019) 'Spatial distributions and sea-to-air fluxes of non-methane hydrocarbons in the atmosphere and seawater of the Western Pacific Ocean', *Science of the Total Environment*. Elsevier B.V., **672**, 491–501.
- Lin, Y. S., Heuer, V. B., Goldhammer, T., Kellermann, M. Y., Zabel, M. and Hinrichs, K. U. (2012) 'Towards constraining H<sub>2</sub> concentration in subseafloor sediment: A proposal for combined analysis by two distinct approaches', *Geochimica et Cosmochimica Acta*, **77**, 186–201.
- Lomond, J. S. and Tong, A. Z. (2011) 'Rapid analysis of dissolved methane, ethylene, acetylene and ethane using partition coefficients and headspace-gas chromatography', *Journal of Chromatographic Science*. Oxford University Press, **49**, 469–475.
- Lu, Y. and Conrad, R. (2005) 'In situ stable isotope probing of methanogenic Archaea in the rice rhizosphere', *Science*, **309**, 1088–1090.
- Macdonald, R. W. (1976) 'Distribution of Low-Molecular-Weight Hydrocarbons in Southern Beaufort Sea', *Environmental Science and Technology*. American Chemical Society, **10**, 1241–1246.
- Martin, W., Baross, J., Kelley, D. and Russell, M. J. (2008) 'Hydrothermal vents and the origin of life', *Nature Reviews Microbiology*. Nature Publishing Group, **6**, 805–814.
- Martínez, G. M. and Renno, N. O. (2013) 'Water and brines on mars: Current evidence and implications for MSL', *Space Science Reviews*, 29–51.
- Mcgenity, T. J. and Sorokin, D. Y. (2018) 'Biogenesis of Hydrocarbons', in Stams, A. J. . and Sousa, D. . (eds) *Biogenesis of Hydrocarbons*, 1–27.

- McInerney, M. J., Sieber, J. R. and Gunsalus, R. P. (2009) 'Syntrophy in anaerobic global carbon cycles', *Current Opinion in Biotechnology*, 623–632.
- McKay, W. A., Turner, M. F., Jones, B. M. R. and Halliwell, C. M. (1996) 'Emissions of hydrocarbons from marine phytoplankton - Some results from controlled laboratory experiments', *Atmospheric Environment*. Elsevier Ltd, **30**, 2583–2593.
- McMellor, S. and Underwood, G. J. C. (2014) 'Water policy effectiveness: 30 Years of change in the hypernutrified Colne estuary, England', *Marine Pollution Bulletin*. Elsevier Ltd, **81**, 200–209.
- Middelburg, J. J., Nieuwenhuize, J., Iversen, N., Høgh, N., Wilde, H. De, Helder, W., Seifert, R. and Christof, O. (2002) 'Methane Distribution in European Tidal Estuaries', *Biogeochemistry*. Springer, 95–119.
- Mode, A. W., Anyiam, O. A. and Egbujie, B. C. (2014) 'The application of chromatographic gas ratio analysis in reservoir fluid evaluation of "Beta" field in the Congo basin', *Journal of the Geological Society of India*, **84**, 303–310.
- Moores, J. E., Gough, R. V., Martinez, G. M., Meslin, P. Y., Smith, C. L., Atreya, S. K., Mahaffy, P. R., Newman, C. E. and Webster, C. R. (2019) 'Methane seasonal cycle at Gale Crater on Mars consistent with regolith adsorption and diffusion', *Nature Geoscience*, **12**, 321–325.
- Nair, H., Summers, M. E., Miller, C. E. and Yung, Y. L. (2005) 'Isotopic fractionation of methane in the martian atmosphere', *Icarus*, **175**, 32–35.
- National Research Council (2007) *An Astrobiology Strategy for the Exploration of Mars*. Washington, D.C.: The National Academies Press.
- Nedwell, D. B., Embley, T. M. and Purdy, K. J. (2004) 'Sulphate reduction, methanogenesis and phylogenetics of the sulphate reducing bacterial communities along an estuarine gradient', *Aquatic Microbial Ecology*, **37**, 209–217.

Nedwell, D. B., Underwood, G. J. C., McGenity, T. J., Whitby, C. and Dumbrell, A. J. (2016) 'The Colne Estuary: A Long-Term Microbial Ecology Observatory', in *Advances in Ecological Research*. Academic Press Inc., 227–281.

Oikawa, P. Y. (2016) 'Peer review report 1 On "Comparison of CO<sub>2</sub>, CH<sub>4</sub> and N<sub>2</sub>O soil-atmosphere exchange measured in static chambers with cavity ring-down spectroscopy and gas chromatography"', *Agricultural and Forest Meteorology*. Elsevier, **217**, 2.

Oremland, R. (1988) 'Biogeochemistry of methanogenic bacteria', in Zehnder, A. J. . (ed.) *Biology of anaerobic microorganisms*, 641–705.

Oremland, R. S. (1979) 'Methanogenic Activity in Plankton Samples and Fish Intestines : A Mechanism for in Situ Methanogenesis in Oceanic Surface Waters Submitted : Methanogenic activity in plankton samples and fish intestines : A mechanism for in situ methanogenesis in oceanic', *American society for limnology and oceanography*, **24**, 1136–1141.

Oremland, R. S., Oremland, S. and Kvenvolden, K. A. (1981) 'Microbial Formation of Ethane in Anoxic Estuarine Sediments', **42**, 122–129.

Oremland, R. S., Whiticar, M. J., Strohmaier, F. E. and Kiene, R. P. (1988) 'Bacterial ethane formation from reduced, ethylated sulfur compounds in anoxic sediments', *Geochimica et Cosmochimica Acta*, **52**, 1895–1904.

Osborn, S. G. and McIntosh, J. C. (2010) 'Chemical and isotopic tracers of the contribution of microbial gas in Devonian organic-rich shales and reservoir sandstones, northern Appalachian Basin', *Applied Geochemistry*, **25**, 456–471.

Oze, C. and Sharma, M. (2005) 'Have olivine, will gas: Serpentinization and the abiogenic production of methane on Mars', *Geophysical Research Letters*, **32**, 1–4.

Polovina, J. J., Howell, E. A. and Abecassis, M. (2008) 'Ocean's least productive waters are expanding', *Geophysical Research Letters*, **35**.

- Porco, C. C. *et al.* (2006) 'Cassini observes the active south pole of Enceladus.', *Science (New York, N.Y.)*. American Association for the Advancement of Science, **311**, 1393–401.
- Postberg, F., Kempf, S., Schmidt, J., Brilliantov, N., Beinsen, A., Abel, B., Buck, U. and Srama, R. (2009) 'Sodium salts in E-ring ice grains from an ocean below the surface of Enceladus', *Nature*. Nature Publishing Group, **459**, 1098–1101.
- Redwood, M. D., Paterson-Beedle, M. and MacAskie, L. E. (2009) 'Integrating dark and light bio-hydrogen production strategies: Towards the hydrogen economy', *Reviews in Environmental Science and Biotechnology*, 149–185.
- Reed, C. J., Lewis, H., Trejo, E., Winston, V. and Evilia, C. (2013) 'Protein adaptations in archaeal extremophiles.', *Archaea (Vancouver, B.C.)*. Hindawi, **2013**, 373275.
- Repeta, D. J., Ferrón, S., Sosa, O. A., Johnson, C. G., Repeta, L. D., Acker, M., Delong, E. F. and Karl, D. M. (2016) 'Marine methane paradox explained by bacterial degradation of dissolved organic matter', *Nature Geoscience*. Nature Publishing Group, **9**, 884–887.
- Riemer, D. D., Milne, P. J., Zika, R. G. and Pos, W. H. (2000) 'Photoproduction of nonmethane hydrocarbons (NMHCs) in seawater', *Marine Chemistry*, **71**, 177–198.
- Rudolph, J. (1995) *The tropospheric distribution and budget of ethane*, *JOURNAL OF GEOPHYSICAL RESEARCH*.
- Saad, K. M., Wunch, D., Deutscher, N. M., Griffith, D. W. T., Hase, F., De Mazière, M., Notholt, J., Pollard, D. F., Roehl, C. M., Schneider, M., Sussmann, R., Warneke, T. and Wennberg, P. O. (2016) 'Seasonal variability of stratospheric methane: Implications for constraining tropospheric methane budgets using total column observations', *Atmospheric Chemistry and Physics*. Copernicus GmbH, **16**, 14003–14024.
- Sakai, S., Imachi, H., Sekiguchi, Y., Ohashi, A., Harada, H. and Kamagata, Y. (2007) 'Isolation of key methanogens for global methane emission from rice paddy fields: A novel isolate affiliated with the clone cluster rice cluster', *Applied and Environmental Microbiology*,

**73**, 4326–4331.

Schmidt, U. and Conrad, R. (1993) 'Hydrogen, carbon monoxide and methane dynamics in Lake Constance', *Limnol. Oceanogr.* **38**, 1214–1226.

Schoell, M. (1980) 'The hydrogen and carbon isotopic composition of methane from natural gases of various origins', *Geochimica et Cosmochimica Acta*, **44**, 649–661.

Schwietzke, S., Griffin, W. M., Matthews, H. S. and Bruhwiler, L. M. P. (2014) 'Global bottom-up fossil fuel fugitive methane and ethane emissions inventory for atmospheric modeling', *ACS Sustainable Chemistry and Engineering*, **2**, 1992–2001.

Simpson, I. J., Andersen, M. P. S., Meinardi, S., Bruhwiler, L., Blake, N. J., Helmig, D., Sherwood Rowland, F. and Blake, D. R. (2012) 'Long-term decline of global atmospheric ethane concentrations and implications for methane', *Nature*, **488**, 490–494.

Solomon, S., Qin, D., Manning, M., Chen, Z., Marquis, M., Avery, K., M. Tignor and Miller, H. (2007) 'Climate Change 2007: The Physical Science Basis. Working Group I Contribution to the Fourth Assessment Report of the IPCC', in.

Steel, E. L., Davila, A. and McKay, C. P. (2017) 'Abiotic and Biotic Formation of Amino Acids in the Enceladus Ocean', *Astrobiology*. Mary Ann Liebert, Inc. 140 Huguenot Street, 3rd Floor New Rochelle, NY 10801 USA, **17**, 862–875.

Steinke, M., Randell, L., Dumbrell, A. J. and Saha, M. (2018) 'Volatile Biomarkers for Aquatic Ecological Research', in *Advances in Ecological Research*. Academic Press Inc., 75–92.

Stolper, D. A., Lawson, M., Davis, C. L., Ferreira, A. A., Santos Neto, E. V., Ellis, G. S., Lewan, M. D., Martini, A. M., Tang, Y., Schoell, M., Sessions, A. L. and Eiler, J. M. (2014) 'Formation temperatures of thermogenic and biogenic methane', *Science*. American Association for the Advancement of Science, **344**, 1500–1503.

Takai, Y. (1970) 'The mechanism of methane fermentation in flooded paddy soil', *Soil Science and Plant Nutrition*. Taylor & Francis Group, **16**, 238–244.

Thebrath, B., Rothfuss, F., Whiticar, M. J. and Conrad, R. (1993) 'Methane production in littoral sediment of Lake Constance', *FEMS Microbiology Letters*.

Vanwonterghem, I., Evans, P. N., Parks, D. H., Jensen, P. D., Woodcroft, B. J., Hugenholtz, P. and Tyson, G. W. (2016) 'Methylophilic methanogenesis discovered in the archaeal phylum Verstraetearchaeota', *Nature Microbiology*, **1**, 16170.

Visschedijk, A. J. H., Denier Van Der Gon, H. A. C., Doornenbal, H. C. and Cremonese, L. (2018) 'Methane and ethane emission scenarios for potential shale gas production in Europe', *Adv. Geosci*, **45**, 125–131.

Wagner, D., Schirmack, J., Ganzert, L., Morozova, D. and Mangelsdorf, K. (2013) 'Methanosarcina soligelidi sp. nov., a desiccation- and freeze-thaw-resistant methanogenic archaeon from a Siberian permafrost-affected soil', *INTERNATIONAL JOURNAL OF SYSTEMATIC AND EVOLUTIONARY MICROBIOLOGY*. Microbiology Society, **63**, 2986–2991.

Waite, J. H., Combi, M. R., Ip, W.-H., Cravens, T. E., McNutt, R. L., Kasprzak, W., Yelle, R., Luhmann, J., Niemann, H., Gell, D., Magee, B., Fletcher, G., Lunine, J. and Tseng, W.-L. (2006) 'Cassini ion and neutral mass spectrometer: Enceladus plume composition and structure.', *Science (New York, N.Y.)*. American Association for the Advancement of Science, **311**, 1419–22.

Webster, C. R. *et al.* (2015) 'Mars methane detection and variability at Gale crater', **347**, 415–418.

Webster, C. R. *et al.* (2018) 'Background levels of methane in Mars' atmosphere show strong seasonal variations', *Science*.

Webster, G., O'Sullivan, L. A., Meng, Y., Williams, A. S., Sass, A. M., Watkins, A. J., Parkes, R. J. and Weightman, A. J. (2015) 'Archaeal community diversity and abundance changes along a natural salinity gradient in estuarine sediments', *FEMS Microbiology Ecology*, **91**, 1–

18.

West, W. E., Creamer, K. P. and Jones, S. E. (2016) 'Productivity and depth regulate lake contributions to atmospheric methane', *Limnology and Oceanography*. Wiley Blackwell, **61**, S51–S61.

Whiticar, M. J. (1999) 'Carbon and hydrogen isotope systematics of bacterial formation of methane', *Chemical Geology*, **161**, 291.

Wolanski, E. and Elliott, M. (2016) 'Estuarine ecological structure and functioning', in *Estuarine Ecohydrology*. Elsevier, 157–193.

Wolfe, G. M. *et al.* (2019) 'Mapping hydroxyl variability throughout the global remote troposphere via synthesis of airborne and satellite formaldehyde observations', *Proceedings of the National Academy of Sciences of the United States of America*. National Academy of Sciences, **166**, 11171–11180.

Wolfe, J. M. and Fournier, G. P. (2018) 'Horizontal gene transfer constrains the timing of methanogen evolution', *Nature Ecology & Evolution*, **2**, 897–903.

Xiao, Y., Logan, J. A., Jacob, D. J., Hudman, R. C., Yantosca, R. and Blake, D. R. (2008) 'Global budget of ethane and regional constraints on U.S. sources', *Journal of Geophysical Research Atmospheres*. Blackwell Publishing Ltd, **113**.

Xie, S., Lazar, C. S., Lin, Y. S., Teske, A. and Hinrichs, K. U. (2013) 'Ethane- and propane-producing potential and molecular characterization of an ethanogenic enrichment in an anoxic estuarine sediment', *Organic Geochemistry*.

Yao, M., Henny, C. and Maresca, J. A. (2016) 'Freshwater bacteria release methane as a by-product of phosphorus acquisition', *Applied and Environmental Microbiology*. American Society for Microbiology, **82**, 6994–7003.

Yung, Y. L. *et al.* (2018) 'Methane on Mars and Habitability: Challenges and Responses', *Astrobiology*. Mary Ann Liebert Inc., **18**, 1221–1242.

Zahnle, K., Freedman, R. S. and Catling, D. C. (2011) 'Is there methane on Mars?', *Icarus*, **212**, 493–503.

## Appendix

Figure A1 shows an unsuccessful calibration curve for purge-and-trap analysis of methane (see chapter 2.2 for full methodological details). No linear response was observed with an increase in methane concentration in the gas bags, leading to the conclusion that methane is not cryogenically enriched on this purge-and-trap system.

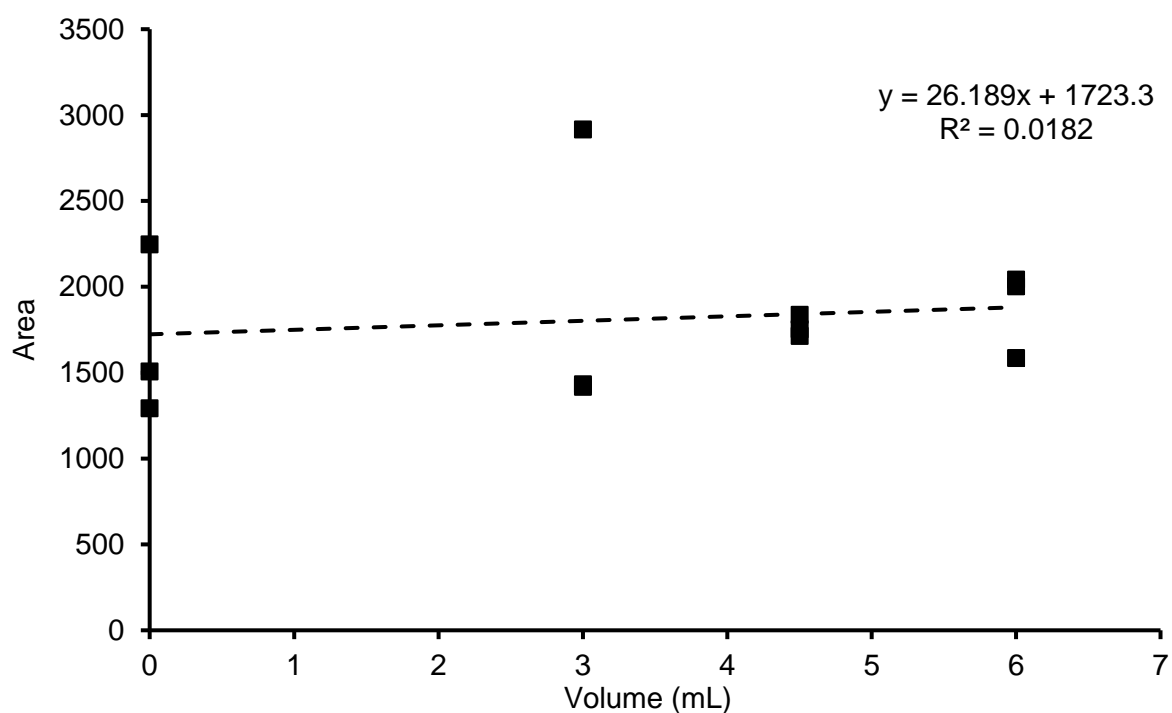


Figure A1: Calibration curve for purge-and-trap analysis of methane, created using gas bags with 0 – 6 mL methane in 3 L of inert nitrogen (equivalent to 0 – 2 ppm methane).

Figure A2 shows an unsuccessful calibration curve for ethane, created using methods detailed in chapter 2.2. This calibration curve was deemed unsatisfactory due to a low  $R^2$  value ( $< .95$ ), prompting a switch from a stainless-steel tubing-based purge-and-trap system to a glass-lined system.

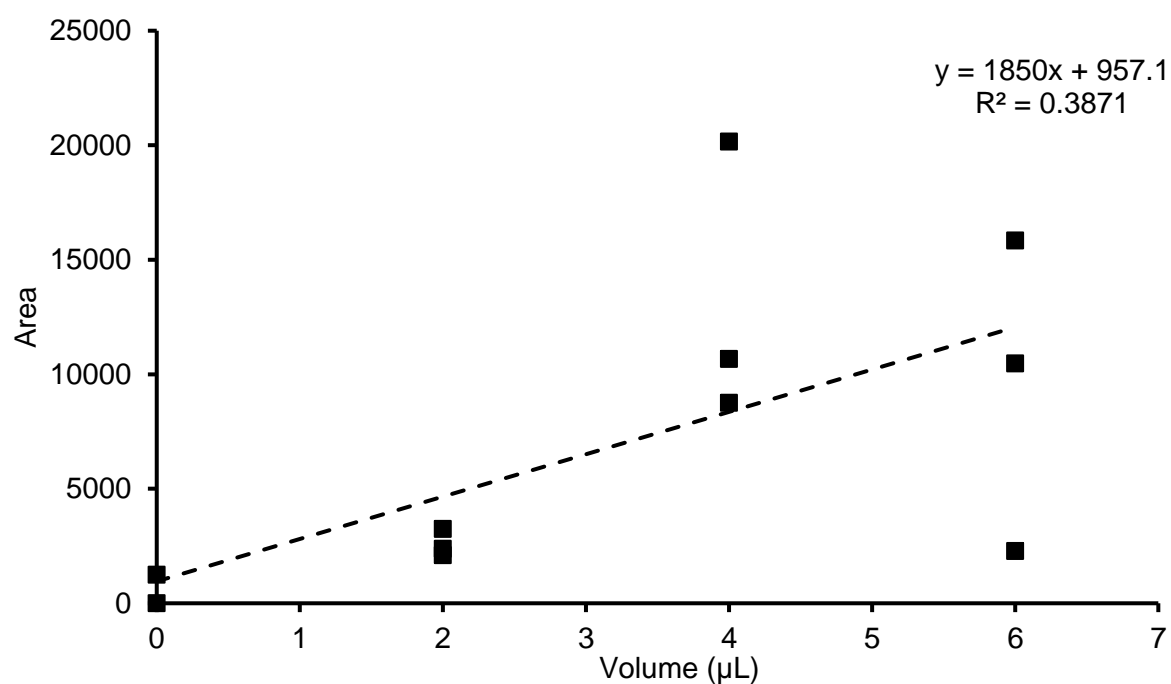


Figure A2: Calibration curve for purge-and-trap analysis of ethane, using a stainless-steel tubing system. Samples of 0 – 6  $\mu\text{L}$  ethane (BOC, >99%) were mixed into 3 L of inert nitrogen in Tedlar™ bags and sucked through the purge-and-trap system at  $60 \text{ mL min}^{-1}$ .

Table A1 shows optimisation for headspace measurements of ethane in environmental samples. An unamended sediment slurry from Hythe sediments was used to optimise the small ethane peak by changing GC-FID settings, to ensure the ethane peak was quantifiable. An optimum regime of 43.0 kPa flow rate in the GC column ramped to 80.0 kPa at 20.0 kPa min<sup>-1</sup> was found, which was then used for all environmental samples.

Table A1: Optimising the ethane peak height to be as above the limit of detection (21.2) and limit of quantification (70.8) as possible by adjusting GC-FID settings. Column flow was set at the initial value for 2.5 minutes, then ramped up to the final value at 20.0 kPa min<sup>-1</sup>.

Column Temperature (°C)	Initial column flow (kPa)	Final column flow (kPa)	Ethane peak height
30	43	60	65
30	43	70	68.3
40	43	80	81.1
40	43	90	75.6
40	43	100	63.1

Table A2 shows retention times from 50  $\mu\text{L}$  samples of standard methane and ethane gases injected into a GC-FID. A major issue with environmental samples is that the methane peak often overshadows the ethane peak due to the massive size discrepancy, leading to optimisation of peak separation (i.e. trying to separate the methane peak from the ethane peak as much as possible). An optimum oven temperature of 40  $^{\circ}\text{C}$  was found, separating the two peaks by 0.8 minutes. An oven temperature of 30  $^{\circ}\text{C}$  had higher separation (1.0 minutes) but standard GC operations cannot reliably occur at 30  $^{\circ}\text{C}$ .

Table A2: Optimising the separation between methane and ethane peaks on the GC-FID by adjusting temperature settings.

Column temperature ( $^{\circ}\text{C}$ )	Methane retention time (mins)	Ethane retention time (mins)
100	2.1	2.5
90	2.2	2.4
80	2.2	2.5
70	2.3	2.7
60	2.3	2.8
50	2.4	3.0
40	2.5	3.3
30	2.6	3.6